SOIL MOISTURE SPATIAL VARIABILITY UNDER FLORIDA RIDGE CITRUS TREE CANOPIES AND IDENTIFYING ALTERNATIVE METHODS OF SCHEDULING IRRIGATION BASED ON TREE CANOPY STRESS

By

LAURA JEANNE WALDO

A THESIS PRESENTED TO THE GRADUATE SCHOOL
OF THE UNIVERSITY OF FLORIDA IN PARTIAL FULFILLMENT
OF THE REQUIREMENTS FOR THE DEGREE OF
MASTER OF SCIENCE

UNIVERSITY OF FLORIDA

2009

Your dedication is typed here. It should begin with the word “To.”
(To my Mom is a typical dedication)

ACKNOWLEDGMENTS

I would like to extend a special thanks to my advisor Arnold Schumann and my committee Jim Syvertsen and Kelly Morgan. I would also like to thank Apogee Instruments for donating the thermal infrared sensors, along with the Hunt Brothers Coop. and the Southwest Florida Water Management District for funding my research. I would also like to thank Marjie Cody, Kevin Hostler, Kirandeep Mann, Sherrie Buchanon, Roy Sweeb, Eric Whaley, and Robert Spitaleri for their help with data collection. A special thanks to my friends and colleagues at the Citrus Research and Education Center in Lake Alfred, Florida for their support from start to finish. Finally, I would like to extend a very special thanks to my parents and grandparents for all of their emotional and financial support over the past 28 years of my life.

TABLE OF CONTENTS

page

LIST OF TABLES

LIST OF FIGURES

Abstract of Thesis Presented to the Graduate School
of the University of Florida in Partial Fulfillment of the
Requirements for the Degree of Master of Science

SOIL MOISTURE SPATIAL VARIABILITY UNDER CITRUS TREE CANOPIES AND IDENTIFYING ALTERNATIVE METHODS OF SCHEDULING IRRIGATION BASED ON TREE STRESS

By

Laura Jeanne Waldo

May 2009

Chair: Arnold W. Schumann
Major: Soil and Water Science

Due to the increasing demand for water in Florida, the supply of water available for irrigation is decreasing and irrigation costs are rising. Conventionally, irrigation is scheduled based on soil moisture status; however the irrigation system, soil type, and canopy interception of both rainfall and irrigation all increase the variability of moisture under citrus tree canopies. Soil moisture measurements were taken 10 cm apart in a 1.5 by 1.5 m grid under citrus trees using a Time Domain Reflectometry probe equipped with 20 cm probe rods. Soil moisture measurements were analyzed using geostatistics in order to create kriging-interpolated spatial maps depicting variations in soil moisture under mature and young citrus trees. The minimum number of TDR sensor measurements required to estimate soil water content in the topsoil with an accuracy of 90% of plant available water (PAW) 95% of the time was 20 to 289. Therefore, due to site specific variation, single point soil moisture measurements were not accurate enough for triggering irrigation to avoid drought stress or leaching. Accurately matching irrigation scheduling with tree-specific needs may require plant based measurements. Several methods for measuring tree canopy stress were tested both in a controlled greenhouse environment and in the field. These methods include infrared radiometers for thermal infrared canopy temperature

measurements, multispectral cameras for water stress index using reflectance, and the GreenSeeker® sensor for measurements of canopy normalized difference vegetation index (NDVI) as an indicator of plant water status. All of the measurements taken were plotted against stem water potential (SWP) as a reference of plant water stress. Results indicate that the thermal infrared radiometer is capable of characterizing water stress using the crop water stress index (CWSI) in a greenhouse setting, however field infrared measurements were less accurate due to instrument sensitivities to wind and low solar radiation levels during cloudy periods. The multispectral camera was able to accurately predict plant water status ($R^2 = 0.90^{***}$) using a ratio of reflectance at the 840 nm and 670 nm wavelengths. Similar results were found using the commercially available GreenSeeker® for NDVI, however the regression analysis showed that while significant, it was less accurate than the multispectral camera ($R^2 = 0.31^{***}$). Therefore, soil moisture spatial variability is too high to accurately measure soil water status using a single point measurement for triggering irrigation, whereas, tree based measurements in the greenhouse using the infrared radiometer could predict water stress using the CWSI, furthermore the multispectral camera and the GreenSeeker® were effective at determining water stress in field trees.

CHAPTER 1
LITERATURE REVIEW

Introduction

Typically, rainfall in Florida exceeds the amount of water lost through evapotranspiration (Morgan, et al., 2006). Annual rainfall, however, is not uniformly distributed throughout the year causing a surplus in the summer (wet) season, and a deficit in the winter and spring (dry) seasons (Morgan, et al., 2006). Due to this fact, supplemental irrigation is necessary to maintain fruit-set and increase yield. Studies have shown that improved management of irrigation is critical in preventing nitrogen and other chemicals from leaching into the surficial aquifer (Morgan, et al., 2006). As a result of these studies, irrigation management is an essential component of the Florida Ridge region's citrus best management practices (BMPs). In order to achieve the desired crop response and reduce irrigation applied, a site-specific irrigation schedule is needed. Site-specific irrigation is matched to the actual crop needs at the smallest manageable unit level (Cohen, et. al., 2005). Identifying the appropriate time to irrigate requires monitoring these needs intensively. Conventionally this has been achieved through soil water monitoring and soil water balance calculations (Jones, 2004). Recently, newer methods of scheduling irrigation have been proposed which use canopy measurements to identify the level of water stress based on tree canopy measurements (Jones, 2004).

Soil-Based Measurements

Conventionally crop water status has been measured using soil-based measurements. These measurements are done by sampling a specific amount of soil and removing the water (direct methods), or by measuring some other soil property such as electrical conductivity (indirect methods) (Muñoz-Carpena, 2004).

Direct Soil Moisture Measurement

There are two types of direct methods for measuring the water content of the soil, thermo-gravimetric and thermo-volumetric methods. The direct thermo-gravimetric method or gravimetric method of measuring the water content of the soil is determined using the difference in the weight before and after drying a soil sample (Charlesworth, 2000). This method measures the water content of the soil by weighing a fresh sample, drying it at 105 °C to obtain the mass of dry soil, then expressing the weight of the water in the soil over the weight of the dried soil (g/g), resulting in the gravimetric water content (Muñoz-Carpena, 2004). One problem with the gravimetric method is the varying density of different soils, which means a unit weight of soil may occupy a different volume (Charlesworth, 2000). In order to compare the different water contents of different soils as well as to calculate the amount of water to add to the soil to satisfy the plants requirements a measure of the soil volumetric water content is needed (Charlesworth, 2000). Likewise, the direct thermo-volumetric method, which is similar to the gravimetric method, uses moist and dry soil weight. However, factoring in the soil's bulk density (mass per unit volume of an undisturbed soil core) and the density of water results in the volume of water over the volume of oven-dried undisturbed sample soil core (m^3/m^3) (Muñoz-Carpena, 2004).

While these methods (gravimetric and volumetric) are accurate and inexpensive, both are slow, taking two days minimum. These direct methods are also destructive since the soil sample must be removed from the field and brought to a lab to be dried in an oven. As a result, repeated sampling from the same location is not possible (Muñoz-Carpena, 2004). These two disadvantages make the direct method of measuring soil moisture impracticable for large scale measurements or for circumstances where soil moisture results are needed quickly, for example, grove irrigation scheduling.

Indirect Soil Moisture Measurement

Similar to the direct methods, there are also two types of indirect methods. The first are volumetric methods, since they measure the volumetric soil moisture, and secondly tensiometric methods, which are those that yield the soil suction or water potential (Muñoz-Carpena, 2004). Indirect methods used to estimate soil moisture involve a calibrated relationship with some other measurable variable. The suitability of these indirect methods is dependent on issues such as cost, accuracy, response time, installation, management and durability (Muñoz-Carpena, 2004).

Indirect methods, both volumetric and tensiometric, are related through a soil water characteristic curve which is specific to a given soil; therefore each soil type must have a different calibration since the methods will not respond the same way for all soil types (Haman and Izuno, 1993). The effectiveness of the indirect measurement device is dependent on the physical properties of the soil, as well as the goal of the soil moisture measurement (Muñoz-Carpena, 2004). While volumetric devices result in a more intuitive quantity, they may not be as useful as some tensiometric devices which relate to the energy that plants have to invest to extract water from the soil, especially in fine textured soils which can hold water tightly to the soil particles making it unavailable for plant absorption (Muñoz-Carpena, 2004). Another important factor for selecting a suitable device for soil moisture measurements is the response time, or time it takes to obtain the result. Some sensors take more time than others because they require the soil moisture to equilibrate with the sensor matrix (Muñoz-Carpena, 2004). Also soil physical properties such as texture may influence the suitability of the sensor due to instrument contact with the soil, and maintenance that may need to be done due to environmental circumstances (Muñoz-Carpena, 2004).

There are several types of volumetric indirect soil moisture measurement methods. These include dielectric, neutron moderation, and ground penetrating radar methods. Also there are

several methods for the tensiometric indirect soil moisture measurements. The tensiometric methods include tensiometers, resistance blocks, heat dissipation, and soil psychrometers.

Dielectric Methods

Dielectric methods estimate the soil water content by measuring the soil bulk permittivity or dielectric constant, Ka_b, which for the time-domain methods determines the velocity of an electromagnetic wave or pulse through the soil (Muñoz-Carpena, 2004). Since soil is made up of different components, which include minerals, air, and water, the value of the permittivity is determined by the relative proportion of each of the components. In addition, since the dielectric constant of water ($Ka_w = 81$) is much larger than that of the other soil constituents (Ka_s = 2-5 for soil minerals and 1 for air), the total permittivity of the soil, or bulk permittivity, is mainly governed by the presence of water (Topp et al., 1980). According to Topp et al. (1980), a common approach to establish the relationship between Ka_b and volumetric soil moisture (VWC) is through the relationship seen in Equation 1-1. The relationship works for most mineral soils and for moisture below 50% (0.5 m^3/m^3). Also the relationship depends on the frequency of the electromagnetic signal sent by the specific device (Topp et al., 1980).

$$VWC = -5.3 \times 10^{-2} + 2.29 \times 10^{-2} Ka_b - 5.5 \times 10^{-4} Ka_b^2 + 4.3 \times 10^{-6} Ka_b^3 \quad (1\text{-}1)$$

Some of these dielectric methods are Time Domain Reflectometry (TDR), Frequency Domain Reflectometry (FDR), Amplitude Domain Reflectometry (ADR), Phase Transmission, and Time Domain Transmission (TDT). All of these methods, except the FDR method, involve an electrical pulse or wave traveling along a transmission line. In the TDR method the pulse travels down and reflects back along the transmission line, whereas in the TDT method the electromagnetic pulse only travels in one direction and has an electrical connection at both ends rather than at a single end (Muñoz-Carpena, 2004). In the ADR method the electromagnetic pulse that is traveling along the transmission line will encounter an area with different impedance

in which part of the wave will be reflected back to the transmitter; as the reflected wave interacts with the incident wave it will change the amplitude of the wave along the transmission line (Wijaya et al., 2002). Similarly in the phase transmission method a sinusoidal wave will show a phase shift relative to the phase at the origin after having traveled a fixed distance along a transmission line (Muñoz-Carpena, 2004). Unlike the methods mentioned previously, the FDR method uses a soil capacitor (the soil between two electrodes) together with an oscillator to form an electrical circuit; changes in the soil moisture can be detected by changes in the circuit operating frequency (Robinson et al., 1999).

Many of these methods are affected negatively by high salinity conditions in the soil. The conditions could be as a result of fertilization or from the use of saline irrigation water. In either case this could lead to an underestimation of the water needed for the trees, and ultimately result in a reduction of the yield. Another problem with many of these methods is the small volume of soil measured for water content. For example, some TDR sensors have a sensing volume along their length defined by only a three centimeter radius, while the ADR method can have a sensing volume as little as 4.4 cubic centimeters (Muñoz-Carpena, 2004). Since the phase transmission and the TDT methods have larger volumes of soil that are measured they also require permanent installation, which disrupts the soil profile and leads to inaccurate measurements due to the channeling of water around the sensor or different soil densities around the sensor that are not representative of the area in question.

Two additional volumetric field methods include ground penetrating radar (GPR) and electromagnetic induction (EMI) (Muñoz-Carpena, 2004). GPR is based on the same principle as TDR; however, it does not require any direct contact between the soil and the sensor. GPR is mounted on a vehicle or a sled close to the soil surface and has the potential of providing rapid,

non-disturbing, soil moisture measurements over a large area (Davis and Annan, 2002). EMI is specifically suited for measurements over large areas. EMI uses two antennae to transmit and receive electromagnetic signals that are reflected by the soil (Dane and Topp, 2002). A problem with EMI is that it does not measure water content directly, but through soil electrical conductivity. As a result, a known calibration relationship between the sensor and the soil is needed, which is site specific and can not be assumed (Dane and Topp, 2002).

Tensiometric Soil Moisture Measurement

Unlike dielectric measurements where the water content is measured, in the tensiometric methods the soil water matric potential is measured. The matric potential of a soil includes both the capillary and adsorption effects of the soil. All of the tensiometric methods include a porous material placed in contact with the soil, which allows water entry. The basic principle of this method is that in a dry soil the water will be removed from the porous medium, and in a wet soil water will travel into the porous material (Charlesworth, 2000). Due to the fact that this method measures the matric potential of the soil, a site specific soil calibration is not needed, however the major drawbacks to this method are permanent installation and the periodic maintenance that is required (Muñoz-Carpena, 2004).

As with tensiometers; resistance blocks, heat dissipation, and soil psychrometers all employ porous material which allows the movement of water. Tensiometers and soil psychrometers are the most common instruments for the measure of the energy status of a soil (Jones, 2007). While tensiometers directly use the soil matric potential, resistance blocks use electrodes within the porous material for measurement based on electrical resistance (Charlesworth, 2000). Along with the use of a porous medium, heat dissipation also makes use of the thermal conductivity of a dry soil versus that of a wet soil (Muñoz-Carpena, 2004). Heat capacity is the amount of heat energy needed to increase the temperature of a quantity of water

by one degree Celsius (Charlesworth, 2000). The soil psychrometer utilizes a porous medium for the flow and entry of moisture; however it measures the relative humidity in a chamber as a result of vapor movement (Campbell and Gardner, 1971). One advantage to these methods is that they are less susceptible to high salt levels in the soil. Unlike tensiometers and resistances blocks, which can require more maintenance, heat dissipation requires very little maintenance (Muñoz-Carpena, 2004). A problem with tensiometric methods, like the volumetric methods, is the generally small sensing volumes in some methods and the high soil disruption of the other methods; both of which could lead to either under or over estimation of soil water and result in over or under irrigation.

While a drawback to some of these sensors is the small sensing volume or sphere of soil, which only allows for an accurate reading from very near the probe location, the sensors that have a larger sensing volume have the drawback of needing to be permanently installed and thus disturbing the soil profile during installation. As a result of some of these drawbacks and disadvantages, some new methods have been identified that rely on measurements of tree canopy water stress rather than soil moisture measurements.

Tree Based Measurements

Several methods of measuring crop water stress have been tested for accuracy in measuring plant water status. One of these methods is crop temperature measurement by thermal infrared thermometers, which have been found to be reliable in some crops as well as non-invasive. Another method tested canopy reflectance using multispectral cameras, which utilize a ratio of the canopy reflectance at two specific wavelengths.

Canopy Temperature Measurements

Plant temperature has long been recognized as an indicator of water availability (Jackson et al., 1981). Until thermal infrared thermometers became available, most plant temperature measurements were made with contact sensors on or embedded in leaves (Jackson et al., 1981). The theory behind the use of canopy temperature is that for any given environmental conditions, the leaf or canopy temperature is directly related to the rate of evapotranspiration from the canopy surface (Leinonen and Jones, 2004). Therefore, as plants transpire the temperature of the canopy is lowered by evaporative cooling, effectively making the canopy temperature cooler than the air temperature. However, when a plant is water stressed, transpiration becomes limited which results in an increase in temperature that can match or exceed that of the air. The usefulness of canopy temperature as a measure of crop water stress was recognized in the 1960s (Möller et al., 2007). Jackson (1981) derived the use of canopy temperature minus air temperature (Tc – Ta), from the energy balance for a crop canopy (Equation 1-2).

$$Rn = G + H + \lambda E \quad (1\text{-}2)$$

Where Rn is the net radiation (W/m^2),
G is the heat flux below the canopy (W/m^2),
H is the sensible heat flux (W/m^2) from the canopy to the air,
λE is the latent heat flux to the air (W/m^2), and
λ is the heat of vaporization

Hope and Jackson (1989) used Tc – Ta, of a wheat crop, as an index of crop water status. The difference (Tc – Ta or ΔT) is also called the "stress-degree-day" when the ΔT is summed over a period of time. Later Tc – Ta and vapor pressure deficit (VPD) data for several crops showed a linear relationship for well watered crops under clear sky conditions (Jackson et al., 1981). Jackson et al. (1988), identified the use of upper and lower limits for calculating the crop water stress index (CWSI) (Equation 1-3), and described the purpose of the upper (ΔT_{UL}) and lower (ΔT_{LL}) limits was to form bounds by which the measured temperature can be normalized.

$$CWSI = ((\Delta T - \Delta T_{LL})/(\Delta T_{UL} - \Delta T_{LL})) \quad (1\text{-}3)$$

According to Monteith and Unsworth (2008), there is a dependence of transpiration rate on radiation and vapor saturation deficit. When leaves are in their natural environment, stomatal aperture depends strongly on solar radiation; in the absence of light, stomata are usually closed, making transpiration effectively zero (Monteith and Unsworth, 2008). There is also substantial evidence both from the field and from work in controlled environments which reveals that many plants close their stomata as saturation deficit or VPD increases, which is presumably a mechanism for conserving water (Monteith and Unsworth, 2008).

Multispectral Imagery

Electromagnetic radiation that is reflected or emitted from the Earth's surface can be recorded by a sensor from the ground, aircraft, or satellite (Curran, 1983). Today an increase in knowledge of the way in which electromagnetic radiation interacts with our environment, has enabled scientists to use such remotely sensed data to determine the amount of soil moisture in a field or the amount of suspended sediment in estuarine waters (Curran, 1983).

Some of the solar irradiance that is impinging upon a vegetation canopy is reflected, while the rest is either transmitted and/or is absorbed (Curran, 1983). The intensity with which radiation is reflected at any particular wavelength is dependent on both the spectral properties and also the area of the leaves, substrate, and shadow (Curran, 1983). Leaves usually reflect weakly in the blue and red wavelengths due to the absorption by photosynthetic pigments, and likewise they reflect strongly in the near-infrared (NIR) wavelengths due to cellular refraction. The most widely used green vegetation indices are formed with data from discrete red and NIR bands (Elvidge and Chen, 1995). A ratio called the normalized difference vegetation index (NDVI) or Vegetation index (Iv) (Equation 1-4) is one of the more popular (Curran, 1983).

$$Iv = (R_{ir} - R_r)/(R_{ir} + R_r) \quad (1\text{-}4)$$

Where R_{ir} is NIR reflectance and
R_r is red reflectance

Spectrometers with measurement ranges beyond 1000 nm have been used to determine water stress in plants by analyzing reflectance measurements at several key wavelengths called water bands (Dallon and Bugbee, 2003). The most prominent water bands are at 1400 and 1900 nm and reflectance at these wavelengths has been shown to correspond to water content in plant tissue (Dallon and Bugbee, 2003). Unfortunately natural sunlight reaching the surface of the earth has low intensities at these wavelengths due to absorptive filtering by water in the atmosphere. Spectrometers capable of measuring radiation beyond 1000 nm are also considerably more expensive than those measuring in the visible and short wavelength NIR ranges (i.e. 400 – 1000 nm). At the 970 nm wavelength there is another water band, however it has historically been considered too small to accurately measure water stress. Dallon and Bugbee (2003) found that if using an accurate spectrometer that can measure wavelengths up to 1000 nm, accurate estimates of water stress can be measured at the 970 nm water band. In order to test the use of the 970 waveband Dallon and Bugbee (2003) used three indices to analyze the various water bands. The first of the indices used, the reflectance water index, is a ratio between the reflectance at a water band to a nearby reference wavelength that is unaffected by water content variability. The second of the indices used is the band depth analysis, which uses a process called continuum removal where a linear continuum line is approximated across an area of absorption, connecting two unaffected points of the spectrum; and the third of the indices is the first-order derivative green vegetation index (1DGVI), which is based on a complex calculus formula involving integrated derivatives that reduces down to a simple difference between a wavelength within the water band that is subtracted from a reference point wavelength.

Applying a similar index to images taken with a multispectral camera, Schumann et al. (2007) found that by photographing a canopy at specific wavelengths with a multispectral camera can result in a yield index and a canopy stress index. Using a multispectral camera fitted with a filter wheel, Schumann et al. (2007) used grayscale values for each pixel from citrus canopy images taken at 840 nm and 670 nm and applied these pixel values to a ratio of 840 nm / 670 nm.

Hypothesis and Research Objectives

Given that there are several factors which lead to variability in soil moisture, it is possible that using single point measurements will not be sufficient enough to accurately trigger irrigation. As a result, irrigation managers will need to rely on some other method of scheduling irrigation. Thermal canopy temperature measurements and multispectral camera imaging, when applied to tree canopy measurements, have a possibility of detecting plant water stress. Presumably using the tree's canopy for water stress measurements would be more accurate because of the trees ability to integrate water from the entire root system. Using the canopy for measuring stress should remove the possibility for variation due to single soil based measurements.

Hypothesis

- The spatial variability of water in the rootzone under citrus tree canopies at a given time is excessive and limits the use of single-sensor soil moisture data for triggering irrigation events.
- Canopy measurements taken with an infrared radiometer, multispectral camera, or GreenSeeker® can be used to estimate the current water status of a citrus tree with the possibility of being used for irrigation triggering.

Research Objectives

- To investigate the soil moisture variability under citrus tree canopies using a TDR moisture sensor and spatially mapping the moisture results under several citrus trees before and after rain or irrigation.

- To test several alternative methods of measuring tree water stress based on canopy measurements in order to determine if these methods could lead to optimal irrigation scheduling which would effectively supply water to the trees and minimize the leaching of nutrients due to over irrigation.

CHAPTER 2
SPATIAL VARIABILITY OF SOIL WATER UNDER CITRUS TREE CANOPIES IN CENTRAL FLORIDA

Introduction

Irrigation is normally carried out according to recommendations based on potential evapotranspiration, and crop coefficients, with adjustment according to soil moisture and rainfall (Cohen et. al., 2005). Due to the possible spatial variability of soil moisture under a citrus tree canopy it may not be practical to use soil measurements for accurate irrigation scheduling.

As mentioned in Chapter 1, soil moisture is calculated using direct measurements of soil water by weighing and drying a soil sample and indirect measurements which include dielectric and tensiometric methods. The disadvantages of these methods include the amount of time required for the one time sampling from a single point, as in the case of direct measurements, and the small sensing volume, maintenance, and soil disruption of the indirect methods (Muñoz-Carpena, 2004). Sampling a small volume or sphere of soil with indirect methods would not be a problem if the soil moisture was spatially uniform. However, due to several factors the soil moisture under a citrus tree canopy is spatially variable. This spatial variability of soil moisture results from the variability of soil properties both horizontally and with depth, non-uniform interception of rainfall by the tree canopy, micro-topography, and irrigation methods (Cohen et al., 2005). Irrigation methods used in citrus production in Florida include micro-jet, drip, or overhead sprinkler.

Soil types in the Ridge citrus production area consist primarily of highly drained fine sands in the Entisol soil order. The tree canopy affects where rainfall will make contact with the soil (Alva et al., 1999). Rain collects on leaves and branches, running along stems and the canopy edge increasing the affects of rainfall in some areas more than others. Irregularities from irrigation application will cause variability; for example, irrigation nozzles impose a pattern in

the application of the water (Figure 2-1). Irrigation nozzles that are designed to have an evenly wetted area are disrupted by low hanging branches, the tree trunk, and wind, which can affect the wetted pattern on the ground surface. The some of the indirect moisture sensing devices that are available today are adversely affected by the salinity of the soil, either as a result of fertilization or saline irrigation water (Boman and Stover, 2002). As ionic strength in the soil solution increases so does apparent soil water content measured with these sensors. Increased salinity also affects the osmotic potential in the rhizosphere relative to unaffected soil, thus, affecting the uptake of water (Muñoz-Carpena, 2004). These sensors may show that there is adequate water in the soil for the tree to absorb while in reality that moisture may not be sufficient. This is due to the fact that the indirect methods rely on the dielectric constant of the measured media, measuring in essence, the electrical conductivity of the soil, which is strongly affected by ions in solution. The sensor circuit's output in volts or millivolts is converted to soil moisture based on a specific calibration in order to make the measurement useful for moisture sensing. An increase in salts in the soil, due to fertilization or the use of saline irrigation water will increase the electrical conductivity of the soil solution causing the sensor to report more soil moisture than was is actually present in the soil (Boman and Stover, 2002). In order to overcome this problem, moisture sensors would need to be calibrated over all possible combinations or soil water and salinities. The combination of these issues makes it necessary to map the soil moisture under citrus trees to find out whether single point soil moisture measurements are accurate enough to predict the water requirements of a tree without either over or under irrigation.

Hypothesis

The spatial variability of water in the rootzone under citrus tree canopies at a given time is excessive and limits the use of single-sensor soil moisture data for triggering irrigation events.

Objectives

To investigate the soil moisture variability under citrus tree canopies using a TDR moisture sensor and spatially mapping the moisture results under several citrus trees before and after rain or irrigation.

Materials and Methods

A one hectare citrus grove (Block 9B) located at the Citrus Research and Education Center (CREC), in Lake Alfred, Florida was used for this study. According to the Southwest Florida Water Management District's GIS website (2002), the soil found in this block is Candler Fine Sand, 0 to 5 Percent slopes. The Candler series is typically found on the Florida Lake Wales Ridge and consists of excessively drained soils that formed in sandy marine or aeolian deposits (USDA, NRCS, 1990). Six trees were used in this study; three mature trees (average of 21 m^3) and three young reset trees (average of 9.25 m^3). Square grids of plastic mesh measuring 1.5 x 1.5 m were placed under each tree's canopy on the same side as the micro-jet irrigation nozzle (Figure 2-2). Three additional grids were placed over bare soil, to illustrate the effects of irrigation without tree canopy or root interference. Measurements of soil moisture were taken at uniform 10 cm spacing within the grid, totaling 225 sample points per tree. Soil moisture measurements were taken after rainfall events of 6.25 mm and 11.25 mm and after irrigation events of one hour, equivalent to approximately 2.15 mm, and three hours, equivalent to approximately 6.45 mm. A micro-jet irrigation system was used for the irrigation events, with a violet Maxi-jet fill in 360° nozzle delivering 51 L/h and with a wetted diameter of 5.5 m. (Figure 2-4). The soil moisture was measured using a Time Domain Reflectometry (TDR), Field Scout Soil Moisture Meter (Spectrum Technologies, Plainfield, Illinois) with 20 cm probe rods (Figure 2-3).

Since the TDR instrument is an indirect measurement of soil moisture, a site specific calibration was performed to properly calibrate the TRD probe for accurate measurements of volumetric soil water content (VWC). A large (approximately 15 L), representative, sample of soil was removed at the 0-20 cm depth from the field site and dried in the oven at 105°C for 48 hours. Two liters of mixed, dry soil was used for calibration; de-ionized water was added in known increments by volume and mixed thoroughly with the soil. For each water increment, the moistened soil was packed in a 10 cm diameter PVC tube with end cap, compacted to the 2 L fill mark, and measurements were taken with the TDR meter. The TDR periods, in microseconds, were calibrated with the calculated volumetric water contents by linear regression (Figure 2-5). This linear regression was used to convert the microsecond period to volumetric water content (m^3/m^3) for all of the moisture data collected. Since the irrigation water used is high quality and has an EC of 0.38 dS/m no other calibrations for salt sensitivity were conducted. The soil found in the block where measurements will be taken is a Candler Sand, which is a hyperthermic, uncoated Typic Quartzipsamments, which is low in organic matter and excessively drained, making it fairly resistant to salt buildup. Given the soil type and high quality irrigation water an extra calibration for salts will not be necessary. Since the variability of the soil is what is in question, any added variability due to salts added by fertilizer applications during the study will only add to the increased amount of variability.

The moisture measurements were geospatially analyzed using GS+ Geostatistics for the Environmental Sciences (Gamma Design Software, Plainwell, MI). Semivariograms and Kriging analysis was used to measure the extent and nature of the VWC variability within each measured grid area. The data from root zones under the tree canopies were compared with irrigated bare soil in the same grove.

Three types of VWC measurements were taken: 1) soil moisture after several days of drying, 2) soil moisture one hour after one hour of irrigation (2.15 mm) as well as zero hours, four hours, 24 hours, and 48 hours after three hours of irrigation (6.45 mm); and 3) soil moisture immediately after and 20 hrs after 6.25 mm and 11.25 mm of rainfall, respectively. Soil water data from the blank soil grids, which were away from any trees and should have received no interference from tree canopy or root water uptake were used to compare to the soil water data from the root zone of the mature and young trees. After each rainfall or irrigation event, the soil moisture was analyzed geospatially for variability using Isotropic Semivariograms and Kriging interpolation.

Isotropic Semivariograms

GS+ automatically chooses the model that best fits the data being analyzed. The isotropic models used for the analysis of the moisture data that were collected include the Spherical, Exponential, and Gaussian models. All of the models use the same coefficients which include nugget (Co), effective range (A), range parameter (Ao), and sill (Co + C). The nugget (Co), is the y-intercept of the model, and is a measure of the amount of variance due to errors in sampling, measurement, and other unexplained sources of variance (Mulla & McBratney, 2000). The range parameter (Ao) is used in the isotropic variogram to calculate the effective range (A), which is the distance at which samples become spatially independent and uncorrelated with one another (Mulla & McBratney, 2000). At separation distances greater than the range, sampled points are no longer spatially correlated. This means that as a region is being sampled, in order to understand the spatial pattern of a given property, which in this case is soil moisture, it is advisable that the sampling design use separation distances that are at most, no greater than the value for the range parameter of the semivariogram (Mulla & McBratney, 2000). It is preferable that the sample spacing be from one quarter to one half of the range (Mulla & McBratney, 2000).

Finally the sill (Co + C) is the model asymptote. The sill represents spatially-independent variance. Data locations separated by a distance beyond which semivariance does not change (after the model asymptote or sill) are spatially independent of one another (Gamma Design Software, LLC, 2004). Theoretically the sill is equivalent to the variance of the sampled population at a large separation distance if the data have no trend (Mulla & McBratney, 2000).

The Spherical isotropic model (Figure 2-6) is a modified quadratic function for which at some distance (Ao), pairs of points will no longer be autocorrelated and the semivariogram reaches an asymptote or sill (Co + C) (Gamma Design Software, LLC, 2004). GS+ uses Equation 2-1 for Spherical models.

$$y(h) = Co + C\,[1.5(h/Ao) - 0.5(h/Ao)^3] \quad \text{for } h \leq Ao \qquad (2\text{-}1)$$
$$y(h) = Co + C \quad \text{for } h > Ao$$

Where:
y(h) = semivariance for interval distance class h,
h = the lag distance interval,
Co = nugget variance ≥ 0,
C = Structural variance ≥ Co, and
Ao = range parameter, the effective range A = Ao

The second model which GS+ uses is the Exponential isotropic model (Figure 2-7), which is similar to the Spherical model in that it approaches the sill (Co + C) gradually, but is different from the Spherical model in the rate at which the sill is approached and in the fact that the model and the sill never actually converge (Gamma Design Software, LLC, 2004). GS+ uses Equation 2-2 for Exponential models.

$$y(h) = Co + C\,[1 - \exp(-h/Ao)] \qquad (2\text{-}2)$$

Where:
y(h) = semivariance for interval distance class h,
h = the lag distance interval,
Co = nugget variance ≥ 0,
C = Structural variance ≥ Co, and

Ao = range parameter, in the case of the exponential model the effective range A = 3Ao, which is the distance at which the sill (Co + C) is within 5% of the asymptote.

The third model GS+ uses is the Gaussian isotropic model or hyperbolic isotropic model (Figure 2-8), which is similar to the exponential model in that the model and the sill never actually converge but different in that the model assumes a gradual rise for the y-intercept (Gamma Design Software, LLC, 2004). GS+ uses Equation 2-3 for Gaussian models.

$$y(h) = Co + C\,[1 - \exp(h^2/Ao^2)] \qquad (2\text{-}3)$$

Where:
y(h) = semivariance for interval distance class h,
h = the lag distance interval,
Co = nugget variance ≥ 0,
C = Structural variance $\geq$ Co, and
Ao = range parameter, in the case of the Gaussian model the effective range A = $3^{0.5}$Ao, which is the distance at which the sill (Co + C) is within 5% of the asymptote.

GS+ uses the statistical minimum Residual Sum of Squares (RSS) to select the model that best fits the data. The RSS provides an exact measure of how well the model fits the variogram data. The lower the RSS the better the model fits. GS+ also gives the coefficient of determination (R^2), which provides an indication of how well the model fits the variogram data. The R^2 value is not as precise as the RSS; however it is still useful in evaluating the model fit. Also along with the RSS and R^2, a proportion of C/(CO + C) is calculated. This statistic provides a measure of the proportion of sample variance that is explained by spatially structured variance (Gamma Design Software, LLC, 2004). This value will be equal to1.0 for a variogram with no nugget variance (the curve passes through the origin); conversely it will be equal to 0 where there is no spatially dependent variation at the range specified (Gamma Design Software, LLC, 2004).

Kriging Interpolation

After the semivariogram has been calculated the Kriging interpolation can then be applied to the grid data. Kriging provides a means of interpolating values for points not physically sampled using knowledge about the underlying spatial relationships in the data set (Gamma Design Software, LLC, 2004). The variograms provided this underlying knowledge. Kriging is based on regionalized variable theory and is superior to other means of interpolation because it provides an optimal interpolation estimate for a given coordinate location (Gamma Design Software, LLC, 2004). There are several types which include point and block kriging. For this analysis block kriging was used because the sample points only measure a small area. According to Burrough and MacDonnell (2004), given the large amplitude, short-range variation of many natural phenomena like soil or water quality. Ordinary point kriging would result in many sharp spikes or pits at the data points, which can be overcome by modifying the kriging equations to estimate average values of z for experimental plots of a given area. Block kriging, which was used for the analysis of the moisture data, provides an estimate for a discrete area around an interpolation point (Gamma Design Software, LLC, 2004). Equation 2-4 shows the estimation of value z for block B, which is used in block kriging, while equation 2-5 shows the minimum variance (Burrough & McDonnell, 2004).

$$z(B) = \sum_{i=1}^{n} \lambda_i \bullet z(x_i) \tag{2-4}$$

Where:
z(B) is the variable (z, in this case soil VWC) over block B,
λ_i = weights needed for local interpolation, and
$z(x_i)$ = variable z at known sampling point x at location *i*.

$$\sigma^2(B) = \sum_{i-1}^{n} \lambda_i \bar{\gamma}(x_i, B) + \mu - \bar{\gamma}(B, B) \tag{2-5}$$

Where:
$\sigma^2(B)$ is the estimation of variance for the Block (B),
λ_i is the weight needed for local interpolation,
$\gamma(x_i,B)$ is the estimated average semivariogram between sampled point *i* and the block,
μ is the Langrangian multiplier, and
$\gamma(B,B)$ is the estimated average semivariogram within the block

When these equations (2-4 and 2-5) are used, the resulting smoothed interpolated surface is free from pits and spikes resulting from point kriging (Burrough & McDonnell, 2004).

According to Schmitz and Sourell (2000), it is possible to show how the measurement uncertainty or variability is related to the required number of sensors. Through the use of a 95% confidence level the number of sensors can be determined. Schmitz and Sourell (2000) used an acceptable 10% measurement error of the plant available water (PAW) to create the threshold value which determines the number of sensors or measurements that would be needed. The PAW for the Candler soil present in this experimental grove block is between field capacity, which is 0.085 m^3/m^3 volumetric water content (VWC), and permanent wilting point (PWP), which is 0.02 m^3/m^3 VWC. Therefore, the range for the PAW is 0.065 m^3/m^3 VWC. At 10% of the PAW the threshold will be 0.0065. For added accuracy using a threshold of 5% PAW would set the threshold at 0.00325. A simple confidence interval was calculated with the Excel (Microsoft Corporation, Redmond, Washington) function CONFIDENCE (Equation 2-6). Using the terms alpha, which is equal to 0.05; the standard deviation of a population (σ) of moisture readings, which is the 225 sample points from one individual grid; size, which is the number of sensors that would be required (N). Microsoft Excel uses the standard Confidence Level statistical equation (Equation2-7).

CONFIDENCE(alpha,standard_deviation,size) (2-6)

95% Confidence level = $\pm 1.96\ (\sigma/SQRT(N))$ (2-7)

Results and Discussion

After analysis of the data using GS+, the soil moisture under citrus trees was found to be highly variable. The results from the isotropic semivariograms show a wide range of variability within the tree sizes as well as variation temporally or across the moisture events.

Semivariogram results from the dry, rainfall, and irrigation events (Table 2-1), show the Effective Range (A), in centimeters, which varies from tree to tree. The average A for the young trees for the dry grids (after several days of drying) was 72 cm, while the average A for the mature trees was 50 cm. This difference in effective range could be due to the greater root density under the mature tree and the area of the grid covered by the tree's canopy. The coefficient of variation (CV) for the dry events also shows a range of variation, with the low being 0.26 and a high of 0.56, showing a dispersion of the moisture within the grid and from grid to grid.

After a moisture event such as rainfall of 6.25mm and 11.25mm, the coefficient A varied even more than it did with the dry events. The minimum range for both rainfall events was 16 cm from a mature tree grid, while the maximum A was 104 cm from a young tree grid (Table 2-1). The difference in A can be explained by canopy interception of rainfall causing water to temporarily pool in areas directly below low hanging branches and at the trunk of the tree. The spatial map from the kriging interpolation for this mature tree (Figure 2-9), shows the dark blue areas which represent the areas where water pooled, creating regions of greater moisture (up to 0.3 m^3/m^3 volumetric water content), while leaving other areas nearly dry (as low as 0.02 m^3/m^3 volumetric water content). Root density could also play a role in increasing the variability due to the high active root area under a mature tree. In the case of the large A value from the young tree grid, this could be due to less coverage of the grid by the small tree canopy allowing a more even distribution of rain water to contact the soil. The spatial map from the kriging interpolation

for this young tree (Figure 2-10), shows the larger areas of similar moisture concentrations, with only some minor pooling of rainwater due most likely to soil micro-topography. The CV range for the rainfall events was wide with a low of 0.19 and a high of 0.55 (Table 2-2), and Standard deviation (σ) tended to be higher with the larger rainfall event (Table 2-2) averaging 0.04 m3/m3 for the 11.25 mm rainfall versus the 0.02 m^3/m^3 for the 6.25 mm rainfall event, which indicates that after the increased rainfall the scatter of the data was greater.

Soil moisture after irrigation events also showed a high range of variability from grid to grid. After a one hour irrigation application, A varied from a low of 26 cm to a high of 100 cm, again with the low A being from a mature tree (Figure 2-11) and the high A from the young tree (Figure 2-12). The moisture variability in this situation can be explained by the type of nozzle used, soil micro-topography, root density and canopy size. Figure 2-11, illustrates the ponding locations where the irrigation water pattern was intercepted by low hanging branches, while Figure 2-12 illustrates the nozzle pattern due to increased water infiltration within the pattern of the irrigation spray.

When taking into consideration the irrigation spray pattern on the ground (Figure 2-1), the spray pattern of the irrigation nozzle (Figure 2-4), and the sandy nature of the soil, it stands to reason that a similar pattern would also be obtained through soil moisture measurements. Several of the moisture grids yielded a similar pattern as a result (Figure 2-13). Effective ranges measured one hour after the three hour irrigation event varied a great deal ranging from as low as 34 cm to as high as 116 cm in distance (Table 2-3). Even after 48 hours, the effective range of measured soil moisture is still varied, ranging from a low of 20 cm to a high of 182 cm in distance (Table 2-3).

The variation in effective ranges can also be explained by the interception of irrigation water by low hanging branches, especially within the mature tree grids. In some cases the low hanging branches collected irrigation water and caused pooling of water below these branches, increasing the variability of the wetted pattern. While the blank grids showed moisture concentrated in the nozzle wetting pattern (Figure 2-14), the mature trees showed the moisture in the nozzle wetted pattern as well as in spots where drip apparently was excessive from branches (Figure 2-15). The younger trees also show some branch interception of irrigation (Figure 2-16), but not to the extent that this interference is seen from the mature trees.

The CV data from these grids also confirms that there is excessive spatial variability in measured soil moisture. The minimum CV for the 3 hour irrigation data was 0.23 or 23% and the maximum was 0.48 or 48% (Table 2-4), which shows that not only is the soil moisture variable from grid to grid and event to event, but also within each individual grid.

After calculating the 95% confidence level for the moisture results from each grid, the number of sensors or measurements needed to produce a reliable estimate of the soil moisture status was found to be high. This calculation estimates the minimum number of sensors that would obtain an accurate (acceptable error set at 10% or 5% of the PAW) average soil moisture measurement to reliably trigger irrigation for maintaining the correct soil moisture levels, 95% of the time. Using the confidence function in Excel, the 95% confidence level was calculated for each tree grid using in the calculation the standard deviation of a grid population and the number of sensors (N) and a probability (alpha) of 0.05. The thresholds calculated using both 10 % and 5% of the PAW were used to identify the number of sensors that would be appropriate for the data set. Table 2-5 shows the calculation for one of the dates when the young and mature trees were sampled. The yellow highlight shows the point at which the threshold was reached for the

10% PAW, while the orange highlight shows the point at which the threshold for the 5% PAW was reached. These thresholds establish the number of sensors that would be required for an accurate estimate of the soil moisture.

After all the calculations were completed, at the 10% PAW level, the number of sensors needed after rainfall ranged from a low of 20 measurements, young tree with an evenly distributed rainfall pattern, to a high of 289 measurements, mature tree with a high amount of canopy interference (Table 2-6). After several days of drying the range for 10% PAW was from 34 to 167 measurements (Table 2-6). One hour following an irrigation event of 3 hours (Table 2-7) had a range of measurements that was rather high, with a low of 120 to 168 measurements needed. However 48 hours after the same irrigation event the range of measurements needed was quite a bit lower ranging from 14 to 53 measurements. This shows that a lower number of sensors would be appropriate for triggering the start an irrigation cycle but not for triggering when the appropriate amount of water has been applied, which would require a far greater number of measurements or sensors. Thus, when using soil moisture sensors to trigger irrigation systems, the risk of over-irrigating due to spatially variable soil moisture distribution is higher than the risk of under-irrigating. Using 5% of the PAW would allow for a more accurate application of water, since the soil would not be outside of 5% of the PAW, but would require a substantially large number of measurements or sensors. After rainfall the number of measurements needed at 5% PAW would range from 80 to 1,168 measurements (Table 2-6), which is an unreasonably high number of measurements. Likewise after irrigation the number of measurements needed was also high, with a low of 347 measurements to a high of 675 measurements (Table 2-7). However 48 hours after the same irrigation event, the number of

sensors needed for the 5% PAW was much lower ranging from 54 to 287 measurements, still in many cases unfeasibly high for triggering irrigation.

Soil moisture results indicate high variability of soil moisture under citrus trees after all moisture events as well as after several days drying. These results show that the spatial variability is excessive and makes single point measurement, as is often done for irrigation scheduling, inaccurate. Knowing the best place for a single moisture sensor under a tree canopy for accurate irrigation scheduling is impossible, and would lead to situations of either over or under irrigating trees, which can lead to the problems of nutrient and pesticide leaching as well as possible yield reduction due to water stress, as in the case with under irrigation. Since the aim of the Ridge Citrus BMPs is to reduce the amount of nitrogen reaching the groundwater and eventually the aquifer, more efficient irrigation triggers are necessary, and based on these results, this accuracy will not come from single point soil moisture measurements.

Table 2-1. Geostatistics from GS+ isotropic semivariogram analysis for moisture grid data including several days of drying, rain, and 1 hour of irrigation.

Grid #	Parameter Range (Ao)	Effective Range (A)	Nugget (Co)	Sill (Co+C)	R^2	RSS	C/(Co+C)	Model
Several Days of Drying								
Y1	40	119	2.6	5.9	0.850	0.73	0.563	Exponential
Y2	57	57	11.9	23.8	0.883	7.61	0.500	Spherical
Y3	39	39	1.5	4.4	0.598	1.37	0.662	Spherical
M1	12	36	1.7	12.6	0.812	2.53	0.865	Exponential
M2	12	21	0.8	10.3	0.905	0.90	0.919	Gaussian
M3	93	93	1.4	4.5	0.998	0.01	0.695	Spherical
Rainfall (6.25mm)								
Y1	10	18	0.1	2.1	0.633	0.09	0.947	Gaussian
Y2	93	93	2.3	4.9	0.990	0.05	0.524	Spherical
Y3	100	100	1.0	5.2	0.996	0.05	0.813	Spherical
M1	14	24	1.1	7.4	0.834	1.21	0.856	Gaussian
M2	9	28	0.3	5.0	0.725	0.42	0.944	Exponential
M3	23	68	0.2	2.6	0.998	0.00	0.931	Exponential
Rainfall (11.25mm)								
Y1	13	40	0.7	9.3	0.938	0.59	0.927	Exponential
Y2	72	72	9.3	18.7	0.992	0.40	0.505	Spherical
Y3	60	103	10.6	28.8	0.997	0.89	0.631	Gaussian
M1	12	36	7.6	32.9	0.834	11.30	0.767	Exponential
M2	9	16	1.0	18.1	0.579	4.51	0.945	Gaussian
M3	62	62	4.2	11.4	0.979	0.54	0.634	Spherical
After 1 Hour Irrigation								
Y1	46	46	1.5	11.5	0.983	0.57	0.873	Spherical
Y2	67	67	3.1	15.1	0.990	0.77	0.780	Spherical
Y3	33	100	4.2	12.5	0.990	0.26	0.666	Exponential
M1	17	29	6.1	22.1	0.905	7.23	0.723	Gaussian
M2	9	26	1.8	17.7	0.694	5.25	0.897	Exponential
M3	24	73	1.6	14.1	0.997	0.12	0.890	Exponential

B = Blank, Y = Young tree, M = Mature tree, R2 = Coefficient of determination, RSS = Residual Sum of Squares

Table 2-2. Basic statistical results for moisture grid data including several days of drying, rain, and 1 hour of irrigation.

Grid #	Mean	Median	Mode	Min	Max	σ	SEM	CV
Several Days of Drying								
Y1	0.09	0.09	0.09	0.03	0.28	0.02	0.0016	0.26
Y2	0.08	0.07	0.05	0.02	0.29	0.04	0.0029	0.56
Y3	0.06	0.05	0.05	0.02	0.20	0.02	0.0013	0.34
M1	0.07	0.06	0.06	0.03	0.24	0.03	0.0023	0.49
M2	0.06	0.05	0.06	0.02	0.24	0.03	0.0021	0.52
M3	0.06	0.06	0.07	0.02	0.13	0.02	0.0013	0.33
Rainfall (6.25mm)								
Y1	0.08	0.08	0.08	0.05	0.13	0.01	0.0010	0.19
Y2	0.07	0.07	0.08	0.02	0.13	0.02	0.0014	0.30
Y3	0.07	0.07	0.06	0.02	0.13	0.02	0.0014	0.31
M1	0.07	0.07	0.04	0.02	0.13	0.03	0.0017	0.39
M2	0.06	0.06	0.07	0.02	0.15	0.02	0.0015	0.37
M3	0.06	0.06	0.05	0.02	0.10	0.02	0.0010	0.27
Rainfall (11.25mm)								
Y1	0.11	0.11	0.11	0.05	0.23	0.03	0.0020	0.27
Y2	0.11	0.11	0.07	0.03	0.22	0.04	0.0028	0.37
Y3	0.10	0.09	0.06	0.03	0.27	0.05	0.0032	0.49
M1	0.10	0.08	0.06	0.03	0.32	0.06	0.0038	0.55
M2	0.09	0.08	0.06	0.03	0.31	0.04	0.0029	0.50
M3	0.10	0.11	0.11	0.03	0.20	0.03	0.0022	0.31
After 1 Hour Irrigation								
Y1	0.13	0.14	0.15	0.05	0.24	0.03	0.0023	0.27
Y2	0.10	0.09	0.06	0.04	0.20	0.04	0.0025	0.39
Y3	0.10	0.10	0.11	0.05	0.19	0.03	0.0022	0.32
M1	0.10	0.09	0.05	0.03	0.24	0.05	0.0030	0.46
M2	0.09	0.08	0.05	0.03	0.27	0.04	0.0028	0.47
M3	0.10	0.09	0.05	0.04	0.21	0.04	0.0024	0.37

B = Blank, Y = Young tree, M = Mature tree, σ = Standard deviation, SEM = Standard Error of the Mean, and CV = Coefficient of Variation

Table 2-3. Geostatistics from GS+ isotropic semivariogram analysis for moisture grid data measurements taken 1 h, 4 h, 24 h, and 48 h after irrigation.

Grid #	Parameter Range (Ao)	Effective Range (A)	Nugget (Co)	Sill (Co+C)	R^2	RSS	C/(Co+C)	Model
1 Hour after 3 Hour of Irrigation								
B1	34	34	0.7	10.5	0.935	1.16	0.938	Spherical
B2	34	116	3.8	13.8	0.970	1.15	0.724	Exponential
B3	35	35	0.5	10.2	0.844	3.30	0.948	Spherical
Y1	34	34	0.0	14.2	0.980	0.88	0.999	Spherical
Y2	71	71	2.8	19.3	0.982	2.78	0.856	Spherical
Y3	73	73	6.2	20.6	0.992	0.91	0.699	Spherical
M1	17	50	1.1	20.3	0.995	3.42	0.947	Exponential
M2	12	20	1.6	15.6	0.848	2.68	0.901	Gaussian
M3	95	95	3.5	15.7	0.987	1.31	0.777	Spherical
4 Hours after 3 hour Irrigation								
B1	16	48	0.6	5.9	0.983	0.09	0.892	Exponential
B2	95	95	2.4	6.7	0.993	0.08	0.641	Spherical
B3	22	66	0.6	4.5	0.909	0.41	0.865	Exponential
Y1	30	30	0.2	7.4	0.915	0.63	0.974	Spherical
Y2	28	83	0.0	8.6	0.987	0.34	0.999	Exponential
Y3	86	86	5.1	16.8	0.997	0.31	0.694	Spherical
M1	20	86	1.9	13.6	0.970	1.07	0.862	Exponential
M2	14	41	0.8	8.1	0.976	0.18	0.900	Exponential
M3	60	103	3.2	10.2	0.989	0.47	0.689	Gaussian
24 Hours after 3 hour Irrigation								
B1	39	39	0.2	2.6	0.985	0.02	0.931	Spherical
B2	51	152	0.7	4.3	0.994	0.03	0.832	Exponential
B3	22	67	0.3	2.5	0.934	0.09	0.882	Exponential
Y1	13	23	0.4	4.2	0.932	0.13	0.921	Gaussian
Y2	80	80	1.1	5.0	0.989	0.10	0.780	Spherical
Y3	32	95	0.8	10.5	0.997	0.12	0.925	Exponential
M1	22	38	3.7	8.6	0.917	0.95	0.569	Gaussian
M2	11	32	0.5	5.9	0.874	0.30	0.910	Exponential
M3	115	115	1.4	6.6	0.992	0.14	0.789	Spherical
48 Hours after 3 hour Irrigation								
B1	44	44	0.3	1.7	0.975	0.01	0.832	Spherical
B2	61	182	0.7	3.7	0.987	0.04	0.806	Exponential
B3	49	49	0.6	1.7	0.970	0.01	0.630	Spherical
Y1	12	20	0.3	3.4	0.939	0.05	0.912	Gaussian
Y2	73	73	1.0	3.6	0.967	0.14	0.731	Spherical
Y3	41	122	2.0	9.2	0.992	0.16	0.782	Exponential
M1	15	44	1.0	6.6	0.806	1.15	0.846	Exponential
M2	12	36	0.6	3.1	0.963	0.03	0.811	Exponential
M3	95	95	1.6	4.7	0.997	0.02	0.663	Spherical

B = Blank, Y = Young tree, M = Mature tree, R2 = Coefficient of determination, RSS = Residual Sum of Squares

Table 2-4. Basic statistical results for moisture grid data including measurements taken 1 h, 4 h, 24 h, and 48 h after a 3 hour irrigation application

Grid #	Mean	Median	Mode	Min	Max	σ	SEM	CV
1 Hour After 3 Hour Irrigation								
B1	0.07	0.06	0.04	0.01	0.18	0.03	0.0022	0.47
B2	0.07	0.06	0.03	0.02	0.20	0.03	0.0023	0.48
B3	0.06	0.06	0.05	0.01	0.18	0.03	0.0021	0.48
Y1	0.13	0.14	0.17	0.05	0.21	0.04	0.0025	0.28
Y2	0.10	0.08	0.07	0.03	0.19	0.04	0.0027	0.43
Y3	0.13	0.14	0.15	0.05	0.27	0.04	0.0029	0.32
M1	0.11	0.11	0.07	0.04	0.22	0.04	0.0029	0.38
M2	0.10	0.09	0.07	0.03	0.20	0.04	0.0026	0.38
M3	0.11	0.11	0.06	0.04	0.19	0.04	0.0024	0.35
4 Hours After 3 Hour Irrigation								
B1	0.05	0.05	0.03	0.01	0.18	0.02	0.0015	0.45
B2	0.05	0.05	0.03	0.01	0.14	0.02	0.0016	0.48
B3	0.05	0.05	0.05	0.01	0.11	0.02	0.0013	0.40
Y1	0.11	0.11	0.12	0.04	0.19	0.03	0.0018	0.25
Y2	0.07	0.07	0.05	0.02	0.14	0.03	0.0018	0.36
Y3	0.11	0.11	0.13	0.03	0.21	0.04	0.0026	0.35
M1	0.09	0.09	0.11	0.03	0.19	0.03	0.0023	0.39
M2	0.08	0.07	0.05	0.02	0.14	0.03	0.0019	0.36
M3	0.08	0.08	0.11	0.03	0.15	0.03	0.0019	0.34
24 Hours After 3 Hour Irrigation								
B1	0.04	0.04	0.03	0.01	0.09	0.02	0.0010	0.37
B2	0.04	0.04	0.03	0.01	0.09	0.02	0.0012	0.42
B3	0.04	0.04	0.04	0.01	0.09	0.01	0.0010	0.34
Y1	0.09	0.09	0.09	0.03	0.15	0.02	0.0014	0.36
Y2	0.07	0.06	0.06	0.02	0.11	0.02	0.0014	0.34
Y3	0.09	0.09	0.10	0.03	0.18	0.03	0.0020	0.32
M1	0.08	0.08	0.04	0.01	0.16	0.03	0.0019	0.24
M2	0.07	0.07	0.07	0.03	0.14	0.02	0.0016	0.31
M3	0.07	0.08	0.09	0.02	0.14	0.02	0.0016	0.33
48 Hours After 3 Hour Irrigation								
B1	0.04	0.04	0.03	0.01	0.08	0.01	0.0008	0.30
B2	0.04	0.04	0.04	0.01	0.09	0.02	0.0011	0.38
B3	0.04	0.04	0.04	0.01	0.08	0.01	0.0008	0.29
Y1	0.08	0.08	0.08	0.04	0.14	0.02	0.0012	0.23
Y2	0.06	0.06	0.05	0.02	0.12	0.02	0.0012	0.29
Y3	0.08	0.08	0.08	0.03	0.17	0.03	0.0019	0.33
M1	0.07	0.08	0.08	0.03	0.16	0.02	0.0016	0.33
M2	0.07	0.07	0.08	0.03	0.13	0.02	0.0012	0.26
M3	0.07	0.07	0.07	0.02	0.14	0.02	0.0014	0.30

B = Blank, Y = Young tree, M = Mature tree, σ = Standard deviation, SEM = Standard Error of the Mean, and CV = Coefficient of Variation

Table 2-5. 95% confidence levels calculated for the number of sensors needed for precise soil water estimation

N	Y1	Y2	Y3	M1	M2	M3
1	0.04648	0.08448	0.03767	0.06783	0.06291	0.03920
5	0.02079	0.03778	0.01685	0.03033	0.02814	0.01753
10	0.01470	0.02671	0.01191	0.02145	0.01990	0.01240
20	0.01039	0.01889	0.00842	0.01517	0.01407	0.00877
34	0.00797	0.01449	0.00646	0.01163	0.01079	0.00672
36	0.00775	0.01408	0.00628	0.01130	0.01049	0.00653
50	0.00657	0.01195	0.00533	0.00959	0.00890	0.00554
51	0.00651	0.01183	0.00528	0.00950	0.00881	0.00549
60	0.00600	0.01091	0.00486	0.00876	0.00812	0.00506
80	0.00520	0.00945	0.00421	0.00758	0.00703	0.00438
90	0.00490	0.00890	0.00397	0.00715	0.00663	0.00413
93	0.00482	0.00876	0.00391	0.00703	0.00652	0.00406
100	0.00465	0.00845	0.00377	0.00678	0.00629	0.00392
108	0.00447	0.00813	0.00362	0.00653	0.00605	0.00377
120	0.00424	0.00771	0.00344	0.00619	0.00574	0.00358
130	0.00408	0.00741	0.00330	0.00595	0.00552	0.00344
134	0.00402	0.00730	0.00325	0.00586	0.00544	0.00339
140	0.00393	0.00714	0.00318	0.00573	0.00532	0.00331
146	0.00385	0.00699	0.00312	0.00561	0.00521	0.00324
160	0.00367	0.00668	0.00298	0.00536	0.00497	0.00310
167	0.00360	0.00654	0.00292	0.00525	0.00487	0.00303
180	0.00346	0.00630	0.00281	0.00506	0.00469	0.00292
200	0.00329	0.00597	0.00266	0.00480	0.00445	0.00277
204	0.00325	0.00591	0.00264	0.00475	0.00440	0.00274
360	0.00245	0.00445	0.00199	0.00357	0.00332	0.00207
374	0.00240	0.00437	0.00195	0.00351	0.00325	0.00203
380	0.00238	0.00433	0.00193	0.00348	0.00323	0.00201
400	0.00232	0.00422	0.00188	0.00339	0.00315	0.00196
420	0.00227	0.00412	0.00184	0.00331	0.00307	0.00191
435	0.00223	0.00405	0.00181	0.00325	0.00302	0.00188
500	0.00208	0.00378	0.00168	0.00303	0.00281	0.00175
600	0.00190	0.00345	0.00154	0.00277	0.00257	0.00160
670	0.00180	0.00326	0.00146	0.00262	0.00243	0.00151
674	0.00179	0.00325	0.00145	0.00261	0.00242	0.00151

N = Number of sensors, Y = Young tree, M = Mature tree

Table 2-6. Number of sensors needed, for accurate estimations of soil water, after 95% confidence levels were calculated for each tree grid.

Several Days of Drying		
Grid	10% PAW	5% PAW
Y1	51	204
Y2	167	674
Y3	34	134
M1	108	435
M2	93	374
M3	36	146
Rainfall 6.25 mm		
Y1	20	80
Y2	41	165
Y3	40	158
M1	62	249
M2	47	187
M3	22	88
Rainfall 11.25 mm		
Y1	83	335
Y2	157	635
Y3	210	847
M1	289	1168
M2	170	688
M3	95	383
After 1 Hour Irrigation		
Y1	109	441
Y2	124	499
Y3	100	403
M1	184	744
M2	153	619
M3	115	466

Table 2-7. Number of sensors needed, for accurate estimations of soil water, after 95% confidence levels were calculated for each tree grid.

1 Hour After 3 Hours of Irrigation		
Grid	10% PAW	5% PAW
B1	93	376
B2	106	426
B3	86	347
Y1	130	524
Y2	154	597
Y3	167	675
M1	168	667
M2	139	561
M3	120	486
4 Hours After 3 Hours of Irrigation		
B1	50	202
B2	55	221
B3	36	142
Y1	65	261
Y2	64	257
Y3	135	546
M1	109	441
M2	71	285
M3	73	293
24 Hours After 3 Hours of Irrigation		
B1	22	87
B2	30	119
B3	20	79
Y1	38	153
Y2	38	151
Y3	79	318
M1	72	289
M2	52	209
M3	50	197
48 Hours After 3 Hours of Irrigation		
B1	14	54
B2	24	97
B3	14	57
Y1	31	124
Y2	29	116
Y3	71	284
M1	53	215
M2	28	110
M3	39	157

Figure 2-1. Imposed irrigation wetting pattern from nozzles used in experimental block

Figure 2-2. Example of a tree grid placed under the canopy of a young tree

Figure 2-3. Field Scout TDR100 Soil Moisture Meter used for soil moisture measurements

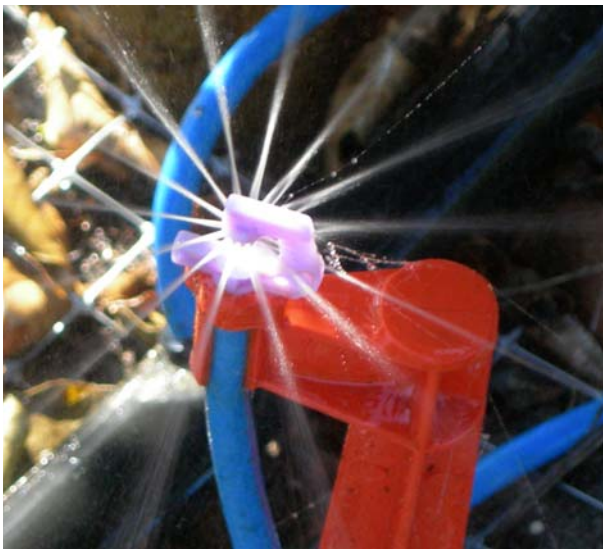

Figure 2-4. Irrigation spray from the micro-jet nozzle used in the experimental block

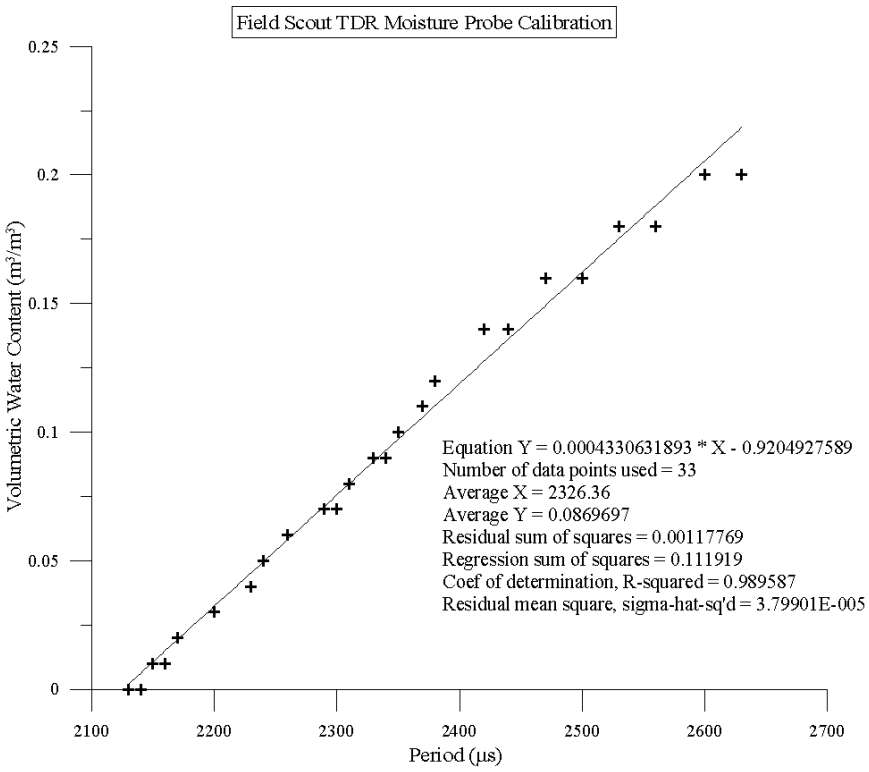

Figure 2-5. Calibration showing linear regression used for conversion from period (µs) to volumetric water content (m^3/m^3)

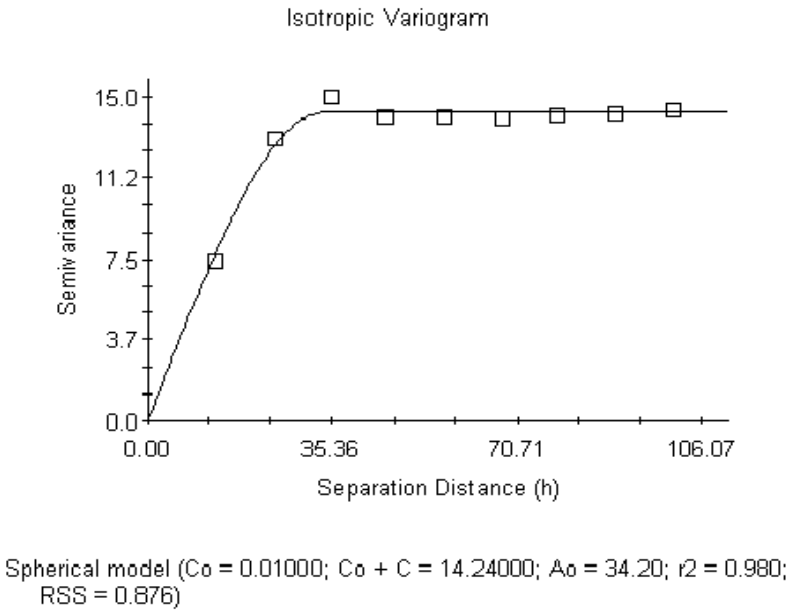

Figure 2-6. Example of the spherical model for isotropic semivariograms (h = cm)

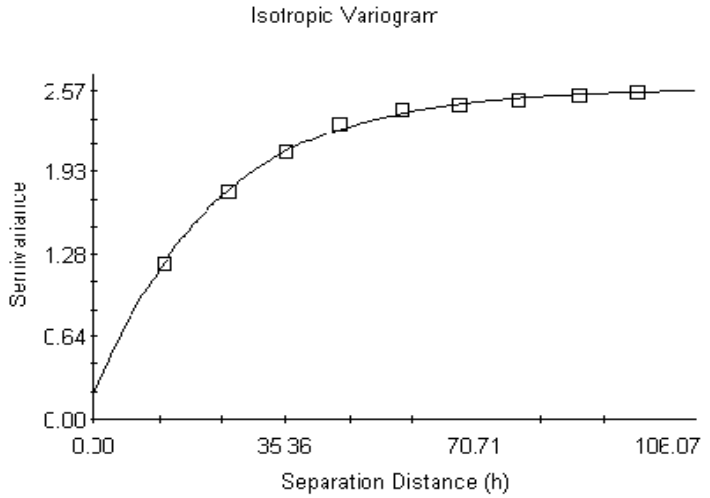

Exponential model (Co = 0.17900 Co + C = 2.59100; Ao = 22.60; r2 = 0.998 RSS = 3.529E-03)

Figure 2-7. Example of the exponential model for isotropic semivariograms (h = cm)

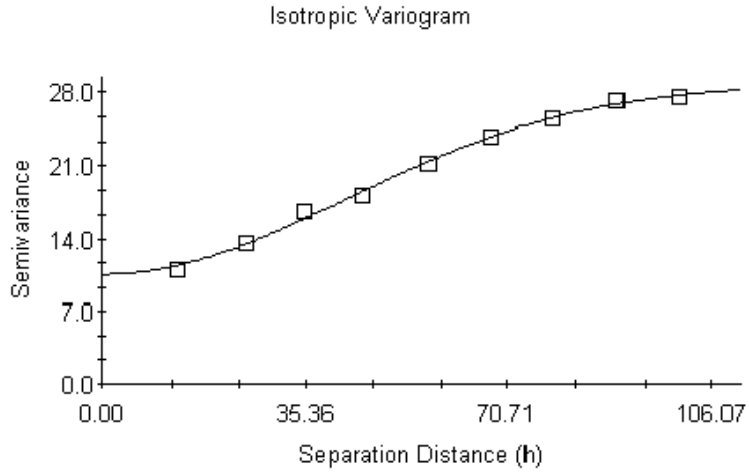

Gaussian model (Co = 10.61000; Co + C = 28.75000; Ao = 59.50; r2 = 0.997; RSS = 0.891)

Figure 2-8. Example of the Gaussian model for isotropic semivariograms (h = cm)

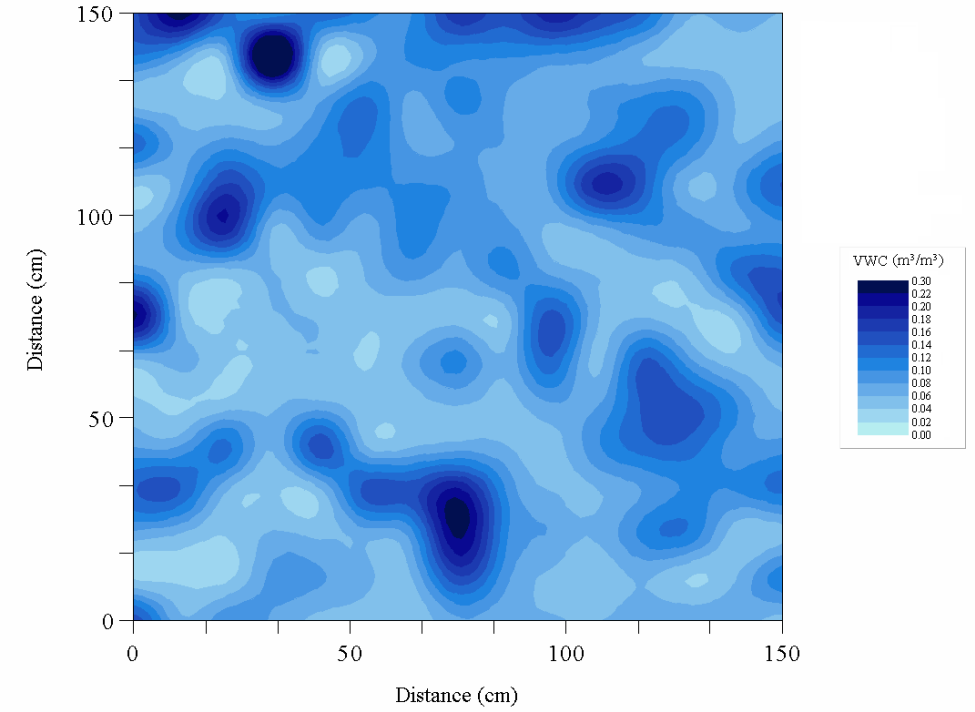

Figure 2-9. Kriging interpolation for a mature tree after rainfall

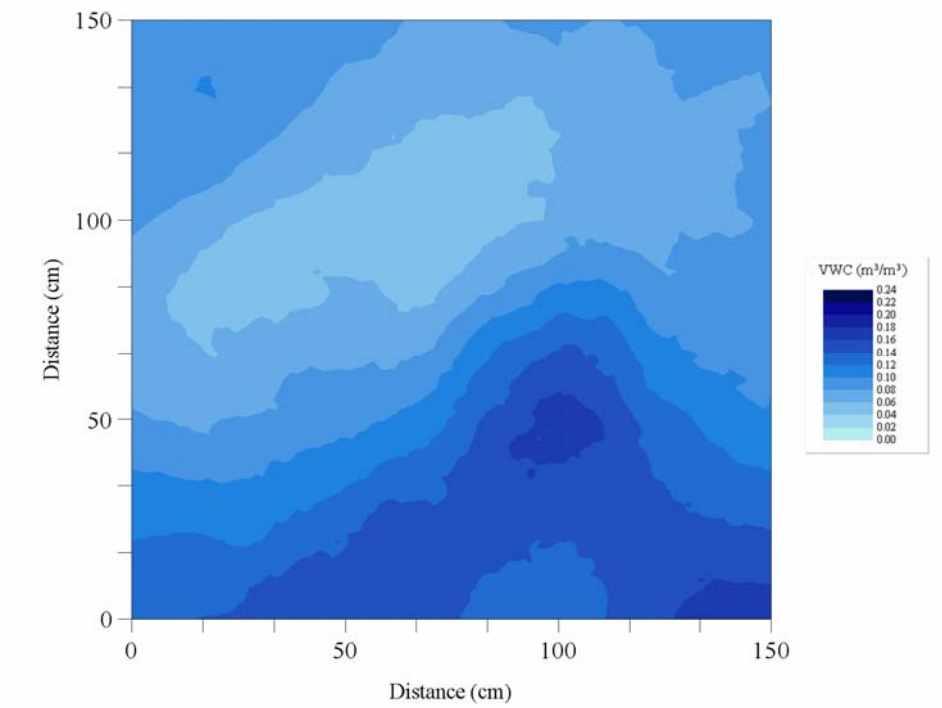

Figure 2-10. Kriging interpolation for a young tree after rainfall

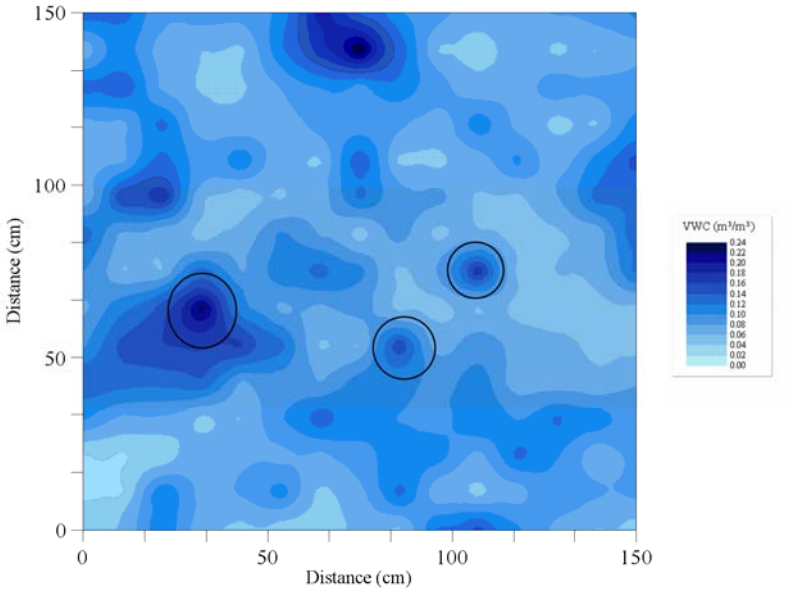

Figure 2-11. Kriging interpolation of a mature tree after 1 hour application of irrigation (circles denote approximate locations of low hanging branches)

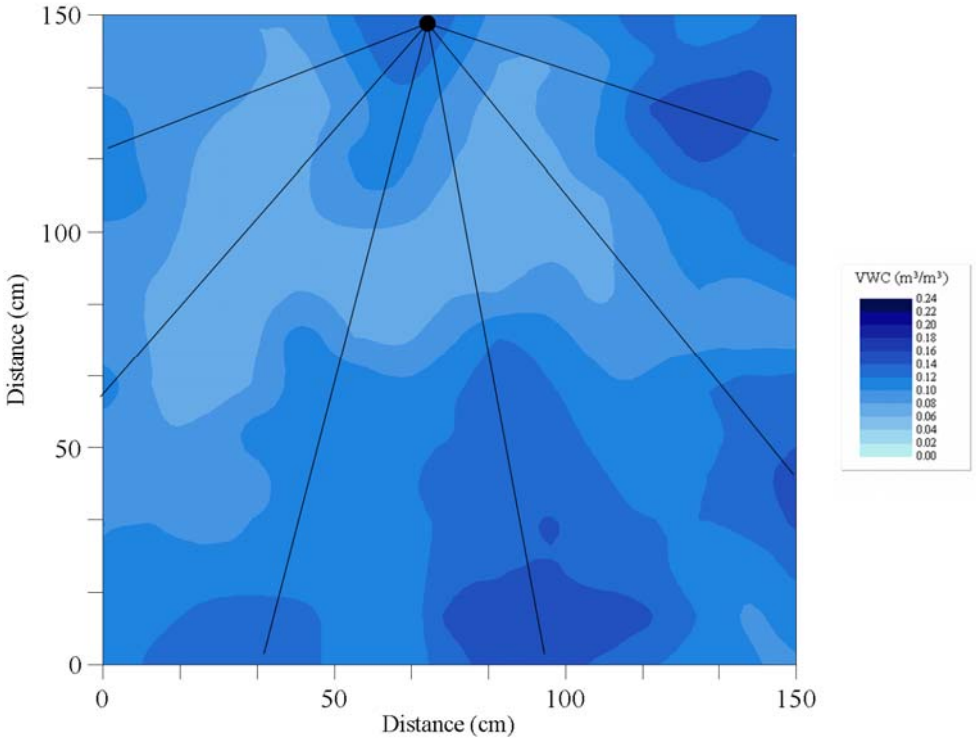

Figure 2-12. Kriging interpolation from a young tree grid following a 1 hour application of irrigation including the overlying pattern of water spray from irrigation nozzle (lines indicate the irrigation wetting pattern)

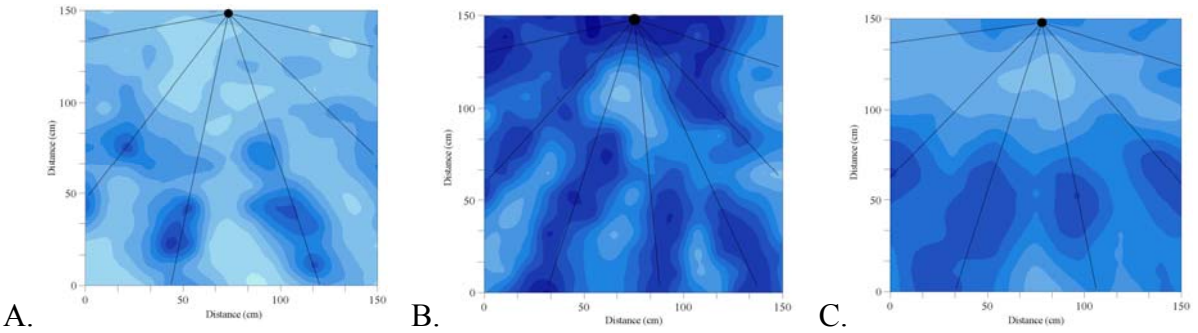

Figure 2-13. Series of Kriging interpolated spatial maps showing irrigation nozzle pattern. A) Moisture results from a blank grid, B) moisture results from a young tree grid, and C) moisture results from a mature tree grid. (lines indicate the irrigation wetting pattern)

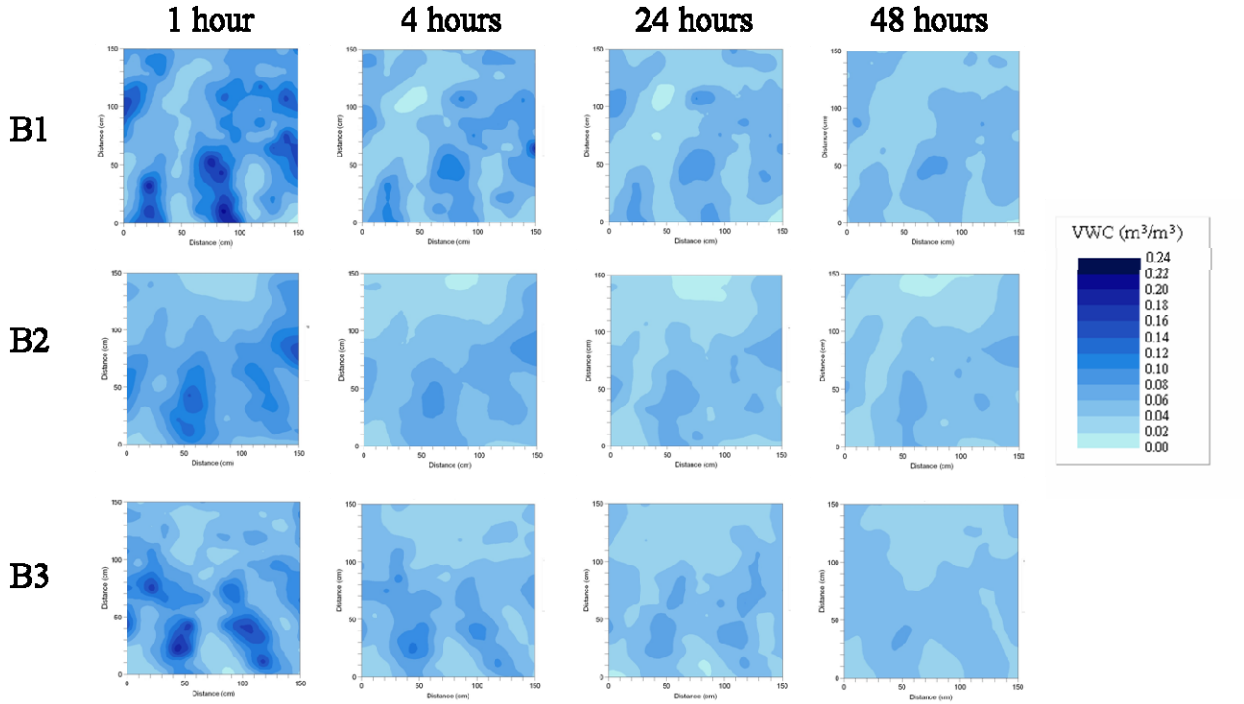

Figure 2-14. Kriging interpolation results from moisture measurements taken from the blank grids 1 hour, 4 hours, 24 hours, and 48 hours after a 3 hour irrigation application.

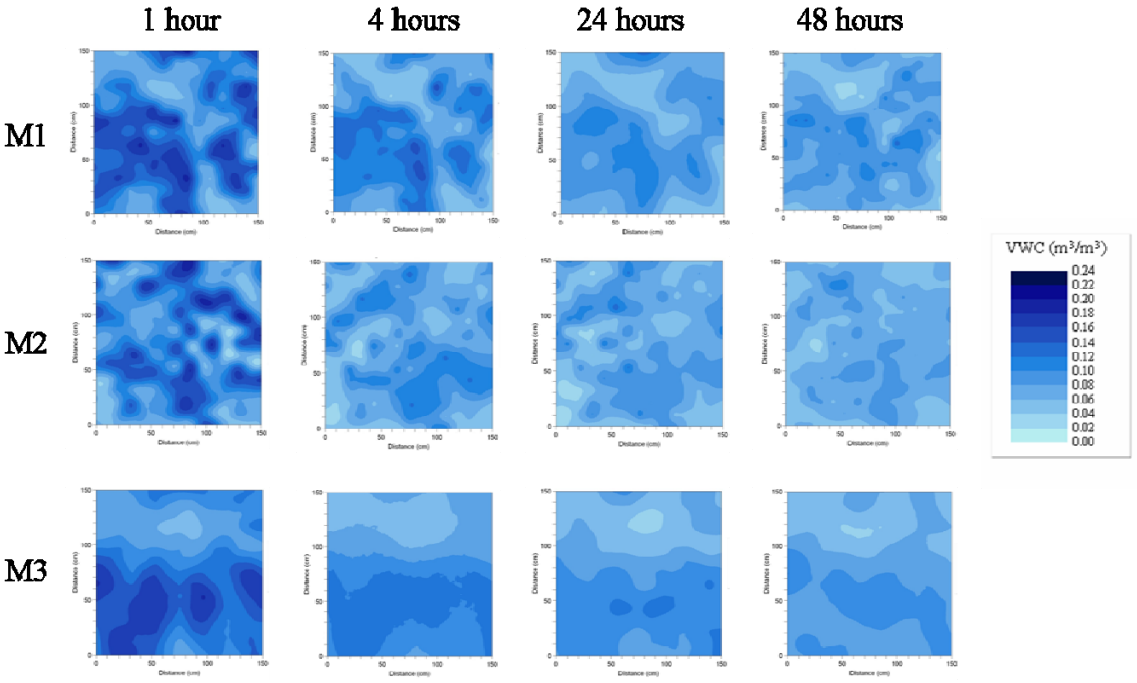

Figure 2-15. Kriging interpolation results from moisture measurements taken from the mature tree grids 1 hour, 4 hours, 24 hours, and 48 hours after a 3 hour irrigation application.

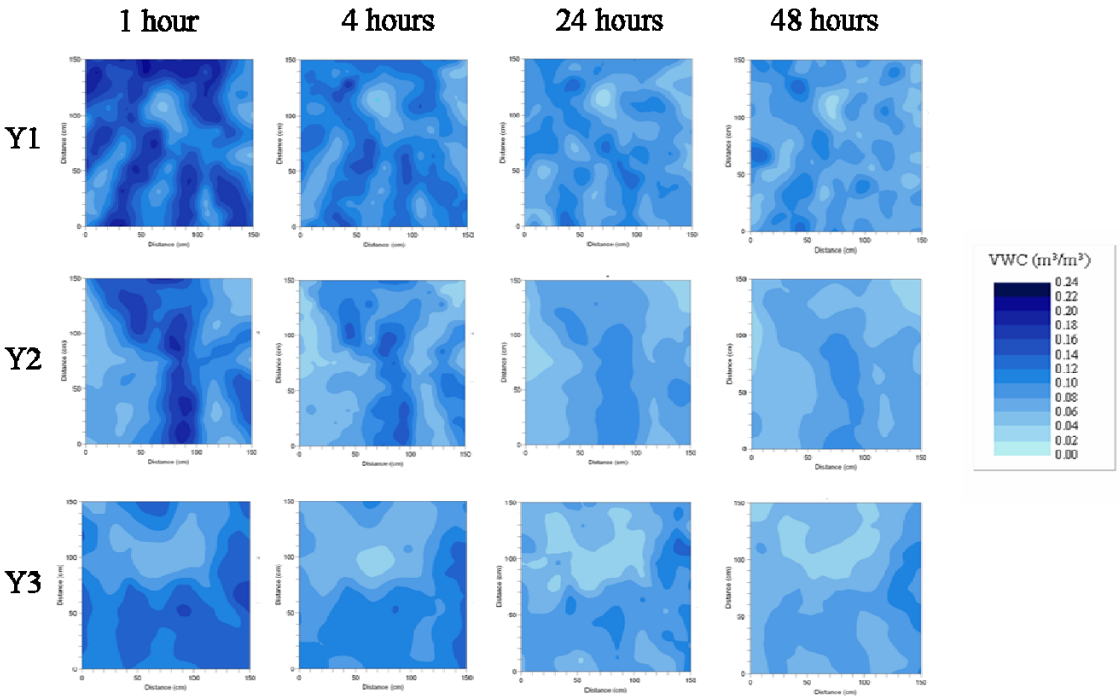

Figure 2-16. Kriging interpolation results from moisture measurements taken from the young tree grids 1 hour, 4 hours, 24 hours, and 48 hours after a 3 hour irrigation application.

CHAPTER 3
IDENTIFYING AND TESTING ALTERNATIVE METHODS OF DETERMINING WATER STATUS FOR IRRIGATION USING TREE CANOPY MEASUREMENTS

Introduction

Irrigation scheduling typically strives to achieve an optimum water supply for maintaining crop productivity with the ultimate aim of soil water content being maintained close to field capacity (Jones, 2004). Even today, many farmers still irrigate by the calendar, applying water whether the crop needs it or not (Jackson, 1982). The farmers that do not irrigated based on the calendar lean towards the use of soil based measurements for irrigation scheduling. However, due to the increasing demand of water for general purposes, the supply of water available for irrigation is decreasing and irrigation costs are rising (González-Dugo et al., 2006). The shortcomings of soil sensors in assessing the water requirements of whole trees were discussed in Chapter 2 of this thesis. As a result, irrigation managers must come up with a method of irrigating that is based on plant specific needs in order to reduce the excess use of water while ensuring the tree has enough to remain productive.

The classical methods of monitoring crop water stress include measurements of soil water content, plant properties, or meteorological variables to estimate the amount of water lost from the plant-soil system during a given period of time (González-Dugo et al., 2006). These methods have been found to be time consuming and in the case of soil moisture methods, too variable for precise irrigation applications with the goal of minimizing water usage.

Several methods for irrigation scheduling are being explored in many different crops, however many of these new methods have not been tested on citrus trees. These plant-based methods include canopy temperature measurements and multispectral imagery.

Canopy Temperature Measurements

Plant temperature has long been recognized as an indicator of water availability (Jackson et al., 1981). Until infrared thermometers became available, most plant temperature measurements were made with contact sensors on or imbedded in leaves (Jackson et al., 1981). As plants transpire the temperature of the canopy is lowered by evaporative cooling, effectively making the canopy temperature cooler than the air temperature. However, when a plant is water stressed, transpiration becomes limited resulting in an increase in temperature that can reach and go beyond that of the air. The usefulness of canopy temperature as a measure of crop water stress was recognized in the 1960s (Möller et al., 2007). Jackson et al. (1981) derived the use of canopy temperature minus air temperature (Tc – Ta), from the energy balance for a crop canopy (Equation 3-1), where R_n is the net radiation (W/m^2), G is the heat flux below the canopy (W/m^2), H is the sensible heat flux (W/m^2) from the canopy to the air, λE is the latent heat flux to the air (W/m^2), and λ is the heat of vaporization.

$$R_n = G + H + \lambda E \quad (3\text{-}1)$$

Hope and Jackson (1989) used Tc – Ta, of a wheat crop, as an index of crop water status. The difference (Tc – Ta or ΔT) when summed over a period of time is also called the "stress-degree-day." For several crops the relationship between Tc – Ta and VPD, for well watered crops under clear sky conditions is linear (Jackson et al., 1981). Jackson et al. (1988), identified the use of upper and lower limits for calculating the crop water stress index (CWSI) (Equation 3-2), and described the purpose of the upper (ΔT_{UL}) and lower (ΔT_{LL}) limits was to form bounds by which the measured temperature can be normalized.

$$CWSI = ((\Delta T - \Delta T_{LL})/(\Delta T_{UL} - \Delta T_{LL})) \quad (3\text{-}2)$$

According to the U.S. Water Conservation Laboratory (2001), the ΔT_{LL} can be calculated using the slope and intercept from a linear regression of a baseline created using measurements of Tc –

Ta from non-stressed plants at varying VPD (Equation3-3) (US Water Conservation Laboratory, 2001).

$$\Delta T_{LL} = \text{intercept} + \text{slope}(VPD) \quad (3\text{-}3)$$

The upper limit represents a fictitious temperature difference that would occur if the canopy were instantly desiccated (Jackson et al., 1988). The upper limit is calculated using the slope and intercept from the regression of the baseline, and includes the saturation vapor pressure (VPs) for a temperature limit that is chosen (Equation 3-4) (US Water Conservation Laboratory, 2001).

$$\Delta T_{UL} = \text{intercept} + \text{slope}(VPs\{Ta\} - VPs\{Ta + \text{intercept}\}) \quad (3\text{-}4)$$

According to Monteith and Unsworth (2008), there is a dependence of transpiration rate on radiation and saturation deficit. When leaves are in their natural environment, stomatal aperture depends strongly on solar radiation; in the absence of light, stomata are usually closed, making transpiration effectively zero (Monteith and Unsworth, 2008). There is also substantial evidence both from the field and from work in controlled environments which reveals that many plants close their stomata as saturation deficit or VPD increases, which is presumably a mechanism for conserving water (Monteith and Unsworth, 2008).

Calculating the VPD of the air is done using the air temperature (°C) and relative humidity (RH). The Saturated vapor pressure (e_s) is calculated using the air temperature (Ta) (Equation 3- 5) (NOAA, Southern Region Headquarters, 2008). Since the RH can be calculated using e_s and the actual vapor pressure (e) (Equation 3-6a), this equation can be modified to calculate the actual (e) using RH (Equation 3-6b) (NOAA, Southern Region Headquarters, 2008). Finally since the VPD is a difference or deficit between the e_s and e, it is calculated by subtraction (Equation 3-7).

$$e_s = 6.11 \text{ x } 10\text{^}((7.5 \text{ x } Ta)/(237.7 + Ta)) \quad (3\text{-}5)$$

$$RH = (e / e_s) \text{ x } 100 \quad (3\text{-}6a)$$

$$e = .01 \times RH \times e_s \quad (3\text{-}6b)$$

$$VPD = e_s - e \quad (3\text{-}7)$$

Multispectral Imagery

Electromagnetic radiation that is reflected or emitted from the Earth's surface can be recorded by a sensor from the ground, aircraft, or satellite (Curran, 1983). Today an increase in knowledge of the way in which electromagnetic radiation interacts with our environment, has enabled scientists to use such remotely sensed data to determine the amount of soil moisture in a field or the amount of suspended sediment in estuarine waters (Curran, 1983).

Some of the solar irradiance that is impinging upon a vegetation canopy is reflected, while the rest is either transmitted and/or is absorbed (Curran, 1983). The intensity with which radiation is reflected at any particular wavelength is dependent on both the spectral properties and also the area of the leaves, substrate, and shadow (Curran, 1983). According to Curran (1983), leaves usually reflect weakly in the blue and red wavelengths due to the absorption by photosynthetic pigments, and likewise they reflect strongly in the near-infrared (NIR) wavelengths due to cellular refraction. The most widely used green vegetation indices are formed with data from discrete red and NIR bands (Elvidge and Chen, 1995). A ratio called the normalized difference vegetation index (NDVI) or Vegetation index (I_v) (Equation 3-8) is one of the more popular (Curran, 1983).

$$Iv = (R_{ir} - R_r)/(R_{ir} + R_r) \quad (3\text{-}8)$$

Where R_{ir} is NIR reflectance and R_r is red reflectance

Spectrometers with measurement ranges beyond 1000 nm have been used to determine water stress in plants by analyzing reflectance measurements at several key wavelengths called water bands (Dallon and Bugbee, 2003). The most prominent water bands are at 1400 and 1900 nm and reflectance at these wavelengths has been shown to correspond to water content in plant

tissue (Dallon and Bugbee, 2003). Unfortunately natural sunlight reaching the surface of the earth has low intensities at these wavelengths due to absorptive filtering by water in the atmosphere. Spectrometers capable of measuring radiation beyond 1000 nm are also considerably more expensive, such as the SVC HR-1024 (Spectra Vista Corp., Poughkeepsie, New York) which costs about $70,000, than those measuring in the visible and short wavelength NIR ranges (i.e. 400 – 1000 nm). At the 970 nm wavelength there is another water band, however it has historically been considered too small to accurately measure water stress. Dallon and Bugbee (2003) found that if using an accurate spectrometer that can measure wavelengths up to 1000 nm, accurate estimates of water stress can be measured at the 970 nm water band. In order to test the use of the 970 waveband Dallon and Bugbee (2003) used three indices to analyze the various water bands. The first of the indices used, the reflectance water index, is a ratio between the reflectance at a water band to a nearby reference wavelength that is unaffected by water content variability. The second of the indices used is the band depth analysis, which uses a process called continuum removal where a linear continuum line is approximated across an area of absorption, connecting two unaffected points of the spectrum; and the third of the indices is the first-order derivative green vegetation index (1DGVI), which is based on a complex calculus formula involving integrated derivatives that reduces down to a simple difference between a wavelength within the water band that is subtracted from a reference point wavelength.

Applying a similar index to images taken with a multispectral camera, Schumann et al. (2007) found that by photographing a canopy at specific wavelengths with a multispectral camera can result in a yield index and a canopy stress index. Using a multispectral camera fitted with a filter wheel, Schumann et al. (2007) used grayscale values for each pixel from citrus

canopy images taken at 840 nm and 670 nm and applied these pixel values to a ratio of 840 nm / 970 nm.

When applied to tree canopy measurements, both thermal and multispectral methods have a possibility of detecting plant water stress. While both the thermal and multispectral procedures have been tested out on several different crops, such as wheat, soy and turf, they have not been tested thoroughly for citrus with the purpose of being used for irrigation scheduling.

Hypothesis

Canopy measurements taken with an infrared radiometer, multispectral camera, or GreenSeeker® can be used to estimate the current water status of a citrus tree with the possibility of being used for irrigation triggering.

Objectives

To test several alternative methods of measuring tree water stress based on canopy measurements in order to determine if these methods could lead to optimal irrigation scheduling which would effectively supply water to the trees and minimize the leaching of nutrients due to over irrigation.

Materials and Methods

Several experiments were carried out to thoroughly test the alternative methods discussed. These methods include thermal infrared canopy measurements and multispectral images of both greenhouse and grove trees. Additional test of the commercially available GreenSeeker® instrument which measures the NDVI of a tree canopy was conducted.

Thermal Infrared Canopy Measurements

Three different experiments were carried out to test the infrared canopy measurements. All three experiments used the precision narrow infrared radiometer (IRR-PN) from Apogee Instruments, Inc. (Roseville, California) (Figure 3-1). The IRR-PN has an 18 degree half angle

and can respond to temperature changes in less than one second. For the temperature range of -10 to 65 °C the sensor has a ±0.2 °C absolute accuracy, ±0.1 °C uniformity, and ±0.05 °C repeatability and uniformity. The field of view for this sensor depends on the angle and distance from the sensor to the canopy. The target temperature reading that is displayed by the sensor is an average of temperatures sensed in the field of view, meaning that all of the leaves in the field of view will be measured, which includes sunlit and shaded leaves. For all of the experiments testing this sensor, only full-sun portions of the tree canopies were used for measurements.

The first of three experiments was done within a greenhouse for controlled environment settings, in order to test the effects of wind on the sensor output. This experiment used 20 non-grafted, Rough Lemon citrus trees (*Citrus jambhiri*) (Figure 3-2). The trees were transplanted from the potting soil and into Candler Fine Sand, 0 to 5 Percent slopes soil taken from a 0-15 cm depth in a citrus grove at the Citrus Research and Education Center, Lake Alfred, Florida. This soil series was used to represent the soil that would typically be found in a Florida Ridge citrus grove. Of the 20 trees, eight were planted with AquaPro direct burial capacitance soil moisture probes (AquaPro Sensors, Ducor, California) (Figure 3-2). The voltage outputs from the sensors were logged using an XR5 data logger (Pace Scientific Inc., Mooresville, North Carolina). Infrared canopy temperature measurements were taken using the IRR-PN which was logged using a CR10X data logger (Campbell Scientific Inc., Logan, Utah). The IRR-PN sensor was placed 30 cm away from, and perpendicular to, a tree canopy, which makes the field of view for the sensor approximately 300 cm^2. The sensor simultaneously measured the air temperature with a built-in transducer which was also logged to the CR10X data logger. Along with infrared measurements, greenhouse climate conditions were also measured. These measurements were logged on an XR5 data logger, and included greenhouse air temperature and relative humidity,

using a TRH-160 temperature/RH probe (Pace Scientific, Inc., Mooresville, North Carolina) and short wave solar radiation using a PYR-PA2.5 high output pyranometer (Apogee Instruments, Inc., Roseville, California).

Measurements with the IRR-PN of the 20 tree canopies were taken along with short wave solar radiation, air temperature and relative humidity while under varying soil moisture conditions, ranging from very dry (0.03 to 0.04 m^3/m^3) to excessively moist (0.20 m^3/m^3) and higher. These measurements were taken both with and without a desktop fan running to test the effect of wind. Wind speed measurements were taken using a Kestrel 3000 Pocket Weather Station (Forestry Suppliers Inc, Jackson, Mississippi).

Using the ΔT method, the air temperatures were subtracted from the canopy temperatures and graphed with soil moisture, stem water potential, and VPD in order to test if the IRR-PN could yield measurements that are related to plant water status.

Stem water potentials were measured using a Scholander-type pressure chamber (PMS instrument, Corvallis, Oregon) (Scholander et al., 1965). According to McCutchan and Shackel (1992), covering a leaf with a reflective bag stops the transpiration of the leaf and eliminates any gradients of water potential within the leaf. When bagged leaves remain attached to the tree for at least 1 hour, the water potential of the leaf would be expected to equilibrate with water potential of the stem and, therefore, be a measurement of the stem water potential (McCutchan and Shackel, 1992). Bags were placed on two leaves per tree in the morning, covered to the petiole attachment point on the stem, and measured for stem water potential in the afternoon, allowing enough time for the water potential in the leaf to equilibrate with the water potential of the stem, and therefore yielding the stem water potential (SWP).

The second experiment that was carried out with the thermal infrared radiometer was used to create the crop water stress index, as well as to see if continuous measurements of Tc – Ta could result in better irrigation triggering. Two of the grove soil potted trees were used. Each tree had an IRR-PN sensor, which was connected to a CR10X (Logan, Utah) data logger, aimed at the edge of the canopy from a 30 cm distance and at a 30 degree angle (Figure 3-4). This angle provides an average of the leaf temperature over the entire field of view for the sensor which is approximately 500 cm^2 (at 30 degrees and 30 cm distance). Measurements were taken every minute for several days to monitor Tc – Ta values over time and as canopy stress increased. Simultaneously measurements of greenhouse air temperature, relative humidity, short wave radiation and volumetric soil water content were also measured every minute. The canopy temperature measurements were compared with the soil moisture status and VPD to test whether the sensor could be used in a stationary setting for tree water status monitoring, with the ultimate result being whether or not it could adequately trigger irrigation.

Research by Jackson (1982) shows that calculations for the crop water stress index can be calculated using the stress-degree-day calculations (Tc – Ta). According to the U.S. Water Conservation Laboratory (2001), the upper (ΔT_{UL}) and lower (ΔT_{LL}) limits for ΔT can be calculated using the vapor pressure deficits and Tc – Ta. In Order to calculate the CWSI the upper limits and lower limits must be known. Calculating the ΔT_{UL} requires knowing the value of ΔT_{LL}. The baseline or ΔT_{LL} can be found by taking measurements from non stressed trees and graphing the Tc - Ta against the VPD. Several days of non stressed measurements were used from the two trees that were placed in front of the IRR-PN sensor in order to find the baseline for the ΔT_{LL}. These measurements from each day were then averaged into hourly periods and plotted to create the baseline linear regression (Figure 3-5). The slope and intercept from this linear

regression were then used to calculate the upper limit (Equation 3-4) and the lower limit (Equation 3-3), which were subsequently used to calculate the CSWI (Equation 3-2). Once the CWSI values were calculated they were averaged and graphed by day along with the irrigation applications. The average for the CWSI uses only the measurements taken between the daylight hours of 10:00 to 15:00 with short wave radiation intensity of greater than 300 W/m^2. This time frame was chosen based on the observations by Idso et al. (1981), which show that for a non-stressed plant, during the daylight hours, the VPD will lie on or near the baseline. Using the results from these data, a vast majority of the measurements for the non-stressed trees fell on or near the baseline during this five hour time frame.

The last experiment with the thermal infrared radiometer used field conditions and 20 trees, 12 of which were mature trees and the remaining eight were young reset trees. A 0.75 ha block of 'Hamlin' orange trees grafted onto Swingle rootstock (block 8A), on the Citrus Research and Education Center (UF, IFAS) campus in Lake Alfred, Florida was used for this experiment. According to the Southwest Florida Water Management District's GIS website (SWFWMD, 2002), the soil found in this block is Candler Fine Sand, 0 to 5 Percent slopes. The Candler series, which belongs to the Entisol soil order, is typically found on the Florida Lake Wales Ridge and consists of excessively drained soils that formed in sandy marine or aeolian deposits (USDA, NRCS, 1990).

Tyvek® HomeWrap® (DuPont, Wilmington, Delaware) plastic fabric was placed under the canopy of six of the mature trees and four of the young trees in order to keep rainfall from penetrating the soil where the majority of the tree roots are located; these trees also had the irrigation nozzle blocked to avoid wetting the soil from irrigation. Of the remaining un-covered trees, three of the large trees and two of the small trees had their irrigation nozzles blocked to

avoid irrigation, and the remaining trees were controls, receiving both irrigation and rainfall. Once visible wilting was observed on the covered soil trees, measurements were taken with the IRR-PN approximately 30 cm away from the tree canopy and held parallel to the surface of the ground at a height of approximately 140cm. This distance and angle yields an average canopy temperature over the field of view which is approximately 300 cm^2. Directly after the measurements for canopy and air temperatures were recorded, the SWPs for the trees were measured. Measurements were taken under both clear and cloudy sky conditions and while the wind was at a minimum. For SWP measurements in this experiment, four leaves on each tree were covered to the petiole attachment point on the stem with plastic bags that were covered with aluminum foil. Bags were placed on the leaves in the morning and measured for stem water potential in the afternoon, allowing enough time for the water potential in the leaf to equilibrate with the water potential of the stem, and therefore yielding the stem water potential (SWP).

Multispectral Camera Imaging

Two different experiments were carried out to test the use of multispectral canopy measurements in identifying tree water stress. Both experiments used the μEye Complementary metal-oxide-semiconductor (CMOS) Monochrome Camera from Imaging Development Systems GmbH (Oberslum, Germany). Attached to the camera is a motorized six filter wheel (Thorlabs, Inc., Newton, New Jersey), which holds six different wavelength filters for 450, 550, 670, 710, 840, and 970 nm.

The procedure for the camera operation and analysis in both experiments follow a similar procedure that was used during an experiment summarized by Schumann et al. (2007). The camera and filter wheel were controlled by software developed by Schumann et al. (2007), running a laptop computer using the USB-2 and RS-232 ports and mounted to a golf cart for portable use in the field. Since the camera is monochrome, the images are in grayscale with pixel

values ranging from 0 to 255, representing the reflectance (R) of that light wavelength from the tree canopy, and a frame size of 480 by 480 pixels. The software was written to analyze each pixel grayscale value and calculate a ratio of the pixel from the 840 nm wavelength image with the corresponding pixel from the 670 nm wavelength image. These values were used because according to Schumann et al. (2007), during a wintertime drought experiment using mature 'Valencia' orange trees on Swingle rootstock, measurements with the multispectral camera that were compared with SWP measurements, yielded a regression analysis of the data that found the pixel grayscale ratio of the reflectance (R) at the 840 nm and 670 nm wavelengths yielded the best canopy stress index (CSI) (Equation 3-9).

$$CSI = R_{(840\ nm)}/R_{(670\ nm)} \quad (3\text{-}9)$$

Since Dallon and Bugbee (2003), found that the 970 nm wavelength was a good estimator of water stress, additional analysis in the laboratory was done using a NIR-128 L near infrared spectrometer (Control Development, Inc., South Bend, Indiana). The absorption spectrum was measured using two leaves from each of the 20 grove soil potted Rough Lemon trees (*Citrus jambhiri*), which were subjected to varying levels of water stress. First, the absorbance at the 670 nm, 840 nm, and 970 nm wavelengths were identified and calculated into CSI ratios of 970/670 nm wavelengths (Equation 3-3) and 840/670 nm wavelengths (Equation 3-4). This was done in an effort to discover if there would be disadvantage of using the 840 nm wavelength, as used in the CSI ratio from Schumann et al. (2007), as apposed to the 970 wavelength, which was used in Dallon and Bugbee (2003). Using the Water Index procedure outlined in Dallon and Bugbee (2003), the ratio of the wavelengths 970 nm and 670 nm was plotted against the ratio of the wavelengths 840 nm and 670 nm. Second, the absorption spectrum of a stressed leaf was compared to that of a non-stressed leaf, which was analyzed by subtraction in an effort to

identify the points along the spectrum of the two leaves where wavelengths varied. Finally, the water stress index ratios of wavelengths 840 nm / 670 nm and 970 nm / 670 nm were plotted against stem water potential measurements, in an effort to determine if there is a disadvantage to using the 840 nm wavelength over the 970 nm wavelength.

The first of the two experiments using the multispectral camera used 20 grove soil potted Rough Lemon (*Citrus jambhiri*) trees. The computer controlled multispectral camera captured images at each of the selected wavelengths. The images were then processed using the wavelengths from the CSI (Equation 3-9). After each tree was imaged, SWP measurements were taken. For this experiment two leaves per tree were covered to the petiole connection point at the stem with plastic lined foil covered bags at least two hours before SWP measurements were taken. The CSI results from this experiment were plotted against the measurements of SWP for each tree in order to test whether CSI calculated from multispectral camera images can adequately determine the water status of a tree for potential use for triggering irrigation.

The second experiment used a 0.75 ha block of 'Hamlin' orange trees grafted onto Swingle rootstock (block 8A), on the same Candler soil described previously. Several trees were selected in this block, including 12 mature trees and 8 young reset trees. In order to induce water stress, Tyvek® HomeWrap® (DuPont, Wilmington, Delaware) was used to cover the soil under the canopies of several trees as described previously (Figure 3-6).

Measurements were taken with the computer controlled multispectral camera only after visible water stress occurred in the trees with Tyvek® covers. During measurements the camera was aimed at a sunlit area of the canopy while the cart was centered in the row middle. The entire field of view for the camera was entirely covered by tree canopy in both the young and mature trees. Immediately after the camera was finished taking the images, SWP was measured.

For this experiment, four leaves on each tree were covered to the petiole attachment point on the stem with plastic lined, foil covered bags. The leaves were covered in the morning and measured for stem water potential in the afternoon, allowing enough time for the water potential in the leaf to equilibrate with the water potential of the stem, and therefore yielding the stem water potential (SWP). In order to test whether the CSI ratio could be used to trigger irrigation the CSI measurements were plotted against the measured SWP from each tree.

GreenSeeker® NDVI

In addition to measurements taken with the multispectral camera, measurements were also taken using the GreenSeeker® RT100 (NTech Industries, Inc., Ukiah, California). Since at any given moment, the amount of solar radiation received at a location on the Earth's surface depends on the state of the atmosphere and the location's latitude, using an instrument that provides it own light source could be an advantage. The GreenSeeker®, unlike the multispectral camera, provides its own light source and is therefore not affected by varying levels of sky irradiance. The output measurement is also different from the multispectral camera in that instead of a water stress index, like the CSI, it uses an NDVI (Equation 3-8), where R_{ir} (NIR) uses the 774 nm wavelength and R_r (Red) uses the 656 nm wavelength. Following similar procedures as in the field experiments using the IRR-PN and multispectral camera the GreenSeeker® was used to test the use of the NDVI as an indicator of plant water stress. The NDVI values calculated were plotted against the average SWP of four leaves per tree.

Results and Discussion

After collecting and analyzing the data the results show that both the infrared radiometer (IRR-PN) and the multispectral camera estimated water stress in citrus trees, but only under specific circumstances. Both sensors worked better under field conditions than in greenhouse conditions. This is probably due to some issues that occurred with the potted citrus trees and the

artificial greenhouse environment. Since the same soil that is found in the field portion of this research was used in the potted trees, moisture control problems became evident. While some trees had adequate drainage, others suffered from poor drainage of the pots which resulted in stress from lack of oxygen to the roots. Field of view for the sensors was another issue that was encountered during the greenhouse experiments. Due to the small size of the canopy for the potted trees there was quite a bit of background noise signal which was introduced into both the infrared readings as well as the photographs taken by the multispectral camera for image processing. This noise resulted in measurement error for the Tc – Ta calculation and the CSI because of the temperature and reflectance of background objects, respectively.

Infrared Canopy Measurements

The results from the first IRR-PN experiment, using 20 greenhouse trees, do not conclude that it could be possible to make an accurate measure of the tree's water stress using the Tc – Ta. When the Tc – Ta values are plotted against the stem water potential (SWP) readings the results do not show a correlation (Figure 3-7), which could be as a result of experimental error. Reduced transpiration, which would result in increased canopy temperature, could be caused by other stresses on the tree canopies. During the experiment there were spider mite infestations, which damaged the leaves, as well as root damage as a result of water logging in the pots. Another possible source of error in the experiment could be from the small canopy size which causes background temperature interference. Since the IRR-PN sensor takes a temperature reading for its entire field of view it is possible the objects in the background not obscured by the tree canopy could cause incorrect temperature readings. Further experimental error could have been introduced with problems encountered while taking stem water potential (SWP) readings. Due to the age of the pressure chamber apparatus, there were several leaks

along the gas lines making it difficult to obtain an accurate measure for the pressures status once the leaf pressure was reached.

When Tc – Ta was plotted against the volumetric water content (VWC) of the soil in the pots, there was no noticeable correlation (Figure 3-8). Experimental error could also have affected these results, with the water saturation occurring near the bottom of the pots. Due to the length of the probe rods (20 cm) and the depth of the soil in the pots (22 cm) it is possible that the soil moisture readings were inaccurate due to the high water status at the bottom of the pot, which at times was near saturation.

Results from the second greenhouse IRR-PN experiment conclude that Tc – Ta can be tracked over a period of time and used to create a threshold for the crop water stress index (CWSI). Long term measurements were taken on two of the greenhouse trees. These measurements included greenhouse air temperature, IRR-PN sensor body temperature, IRR-PN target temperature (canopy temperature), greenhouse relative humidity, short wave radiation, and VWC of the soil in the pot of the tree being measured. When these results are graphed Tc – Ta can be seen for the different times of the day. During daylight hours and while the tree is transpiring the canopy temperature is usually less than the air temperature, however during the night hours, the canopy temperature is higher then the green house air temperature and the IRR-PN sensor body temperature, because there is no photosynthesis and therefore no transpiration, as well as the retention of heat by the plant leaves (Figure 3-9).

The VPD and Tc – Ta data from the long term measurements were used to create the baseline (Figure 3-5) for the CWSI calculations as described in the Materials and Methods section. The slope and the intercept from this baseline were used to calculate the upper and lower limits which are then used to calculate the CWSI (Equations 3-3, 3-4, and 3-2, respectively).

Once the CWSI was applied to the measurements from the long term study and graphed alongside the irrigation applications the trend is apparent (Figure 3-10, A and B). While there are some decreases in the CWSI between the irrigation applications, which are due to environmental conditions such as lower average daily short wave radiation intensity, the general trend is still increasing. Based on these results it is possible that a threshold could be created and used to trigger irrigation. For this experiment water, as irrigation, was applied based on soil moisture status and visual symptoms of water stress. With further research it could be possible to establish a threshold using the CWSI to trigger irrigation, and to test whether this would be more accurate than soil based sensors.

The data from this second greenhouse experiment was also used to compare the Tc - Ta readings taken from the sunny (SWR > 500 W/m^2) and the cloudy conditions (SWR < 300 W/m^2). The data points used in this analysis came from a non-stressed day during the long term measurements, and were from the same period of time (10:00 – 15:00) used in the CWSI analysis. The data from the sunny conditions clearly shows a trend similar to that seen in the non-stressed trees, which was used to create the CWSI. The data from the cloudy conditions illustrates what would be expected, since clouds reflect, absorb and transmit the incoming solar radiation, modifying in this way the amount and spectral quality of the solar radiation reaching the Earth's surface (Alados et al., 1999). The cloud particles are responsible for scattering processes that affect more markedly the shorter wavelengths in the solar spectrum, which include the photosynthetically active radiation spectral range (Alados et al., 1999). Since the clouds reduce the amount of photosynthetically active radiation that reaches the plants, the photosynthesis would be reduced, which in turn, would decrease the amount of transpiration, and therefore increase the canopy temperature, which is reflected by the overall increase in Tc - Ta

(Figure 3-11). This clearly shows that conditions must be sunny during measurements taken with the IRR-PN, since transpiration is reduced under cloudy settings. Taking measurements during periods of low light intensity could give an artificial reading of water stress due to the decrease in transpiration.

Results from the third experiment using the IRR-PN were varied. The large tree data fit to a regression of Tc – Ta versus SWP with a higher R^2 than the small trees ($R^2 = 0.40^*$ and $R^2 = 0.28^{NS}$, respectively), however when placed in the same regression together there was a much poorer fit ($R^2 = 0.19^{NS}$) (Figure 3-12). Measurements were taken on clear sunny days with wind (average wind speed during measurements 1.65 m/s, max wind speed 4.02 m/s) and without wind. After a regression of Tc – Ta to SWP, the results from the measurements taken without wind have a better fit ($R^2 = 0.40^*$) than the results from measurements taken with wind ($R^2 = 0.18^{NS}$) (Figure 3-13). These results agree with the previous research for the Tc – Ta or stress-degree-day measurements done on other crops (Jackson et al., 1988). Even after normalizing the data with the CWSI calculation, which was done using the upper and lower limits from the previous experiment, the results still conclude that the IRR-PN does not yield reliable measurements when used under windy conditions (Figure 3-14).

All of the results from the IRR-PN experiments show that it would be difficult to obtain accurate results from the stress-degree-day or Tc – Ta measurements in the field. The results from the CWSI from the greenhouse however, might yield a reliable system for irrigation triggering of greenhouse trees with more research needed to find the appropriate threshold for the CWSI.

Multispectral Camera Imaging

In order to choose the best ratio of wavelengths for the CSI results, the analysis of the data from the spectrometer experiments was completed. First, after plotting the two ratios against

each other ($R^2 = 0.84^{***}$) the results lead to the conclusion that there is no benefit to using the 970/670 nm ratio over the 840/670 nm wavelength ratio (Figure 3-15). Secondly, based on the results form the subtraction of absorbance spectrums (Figure 3-16, A and B), there is little to no recognizable difference between the wavelengths at 840 nm and 970 nm, which agrees with the water index conclusion that there is no disadvantage to using 840 nm wavelength over 970 nm wavelength. In addition, results from the subtraction show that at the 670 nm wavelength there is an increased difference, indicating that the waveband that is actually indicating stress in the CSI ratio is the 670 nm wavelength. Finally, the results from the regressions of 840 nm / 670 nm and 970 nm / 670 nm (Figure 3-17, A and B) also concludes that there is no disadvantage to using the 840 nm wavelength over the 970 nm wavelength, in fact, the regression of the ratio of 840 nm / 670 nm had a better and more significant fit ($R^2 = 0.23^{*}$) than the ratio of 970 nm / 670 nm ($R^2 = 0.12^{NS}$).

As a result in these experiments the ratio of 840/670 was used in the CSI equation. It is also possible that due to the nonlinear response characteristics of the multispectral camera's image sensor, there is less noise at the 840 wavelength than at the 970nm wavelength, which results in the 840/670 nm ratio yielding better results than the 970/670 nm ratio. The CMOS type sensor used in this camera has a zero response cutoff near 1000 nm which is close to that of the 970 nm wavelength, increasing the possibility of error at this wavelength.

The data from the first experiment to test the multispectral camera was inconclusive due to the same sources of experimental error encountered in the infrared measurements. The sources of error included the overall health of some of the trees. The reduced health is most likely a result of the root rot which was caused by lack of drainage from the pots, or the mite infestations, which damaged the young foliage. Beyond that, experimental error could have been caused by

the small canopy size of the trees used in the experiment. Since the canopies were so small there was quite a bit of background noise that was factored into the crop stress index (CSI) (Figure 3-18). Since during the image analysis, every pixel is used, even the pixels for the greenhouse wall are calculated, resulting in an increased CSI for a tree that is otherwise non-stressed.

Results from the field experiment show a strong connection between the CSI and stem water potential (SWP). CSI from a day of measurements with clear sky conditions and little to no wind shows a strong trend with SWP ($R^2 = 0.90^{***}$) (Figure 3-19). During image processing some of the images were found to cause error due to improper areas of the canopy being captured. During image capture with the multispectral camera the outer uniformly sunlit portions of the canopy are selected (Letter A of Figure 3-19), however during image processing there were two types of error that were encountered, leading to non-uniformly illuminated images; first, interference with young flushes of growth which might artificially increase the CSI due to the light color of the young leaves or because the young leaves tend to wilt before the mature leaves (letters B and D in Figure 3-19); and second, large portions of shaded gaps in the image of the canopy (letters C and E in Figure 3-19). These problems can be seen in the 710 nm wavelength images (Figure 3-20, A-E). The regression created using these data only includes the CSI that were considered not to be such outliers.

Images were also captured for analysis of CSI on a clear day with an average wind speed of 1.65 m/s with gusts up to 4.02 m/s as well as on a cloudy day with little or no wind present. Results show a reduced accuracy of the measurements on the windy day with a regression R^2 of 0.66^{***} (Figure 3-21). This reduced accuracy could be due the movement of the branches as a result of wind from one wavelength image to the next. Since the wavelengths used in the analysis are 670 nm and 840nm, the time between the capture of these images is a few seconds.

During measurements with little to no wind, there would be little to no movement of the canopy, however, on a windy day, the branches would be moving during image capture, resulting in some incorrect pixel ratios. Data collected on a cloudy day also reveal a reduced accuracy of the CSI measurements, with a regression R^2 of 0.44^{**} (Figure 3-22). This could be caused by the reduced reflectance from the canopy as a result of the reduced intensity and altered spectral quality of solar radiation.

Even with the error observed from the windy and cloudy CSI measurements the results from the clear conditions conclude that the multispectral camera could be used for irrigation triggering, however more research would need to be done to identify the threshold for the CSI that would be an indicator of the beginning of water stress. Once this is established it is possible that multispectral camera measurements could be more accurate than soil based measurements because the trees should be the best integrators of available water in the entire root system.

GreenSeeker® NDVI

Finally, NDVI measurements from the GreenSeeker® instrument were plotted against the SWP measurements taken. The results from this regression analysis show that as the water stress decreases the NDVI increases. The calculated NDVI fell between 0.646 for a stressed tree (SWP = -2.84 MPa) and 0.967 for a non-stressed tree (SWP = -1.06 MPa). The regression of NDVI to SWP yielded a linear fit with an R^2 of 0.31^{***} (Figure 3.23). While the results show that a prediction of plant water status could be made, more research would need to be done to find a threshold NDVI for irrigation. Further studies would need to be carried out to determine if this sensor would be accurate enough to trigger irrigation.

Based on the results from all of the experiments carried out to test canopy measurements, it should be possible with further research to develop thresholds that could result in a more accurate trigger for irrigation. In a controlled greenhouse setting, the infrared radiometer could

be used to calculate CWSI which could be used to trigger irrigation after a threshold is established. Based on results from the field studies, the multispectral camera and GreenSeeker® outperformed the infrared radiometer; however thresholds would still need to be identified to determine the proper CSI or NDVI values that would be used to trigger irrigation.

Figure 3-1. Apogee Instruments Inc., IRR-PN Infrared Radiometer

Figure 3-2. 20 Rough Lemon trees, planted in potted grove soil used for greenhouse experiments

Figure 3-3. Aqua-pro capacitance soil moisture probe used for soil moisture monitoring

Figure 3-4. IRR-PN on ring stand pointed at tree canopy during long term measurements.

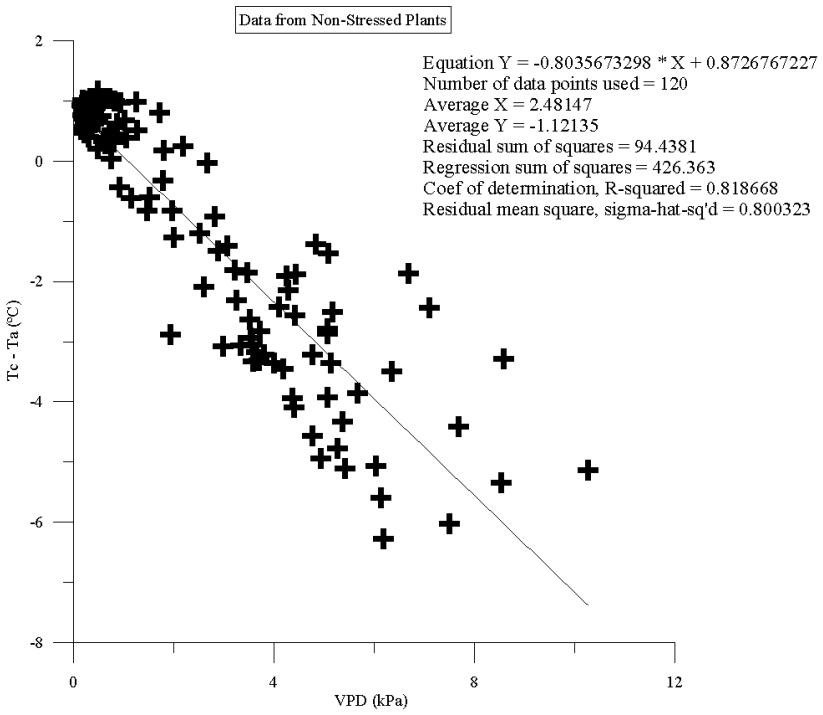

Figure 3-5. Regression analysis from non-stressed tree data for baseline or lower limit (ΔT_{LL}) calculation

Figure 3-6. Soil covered with Tyvek® HomeWrap® (DuPont, Wilmington, Delaware)

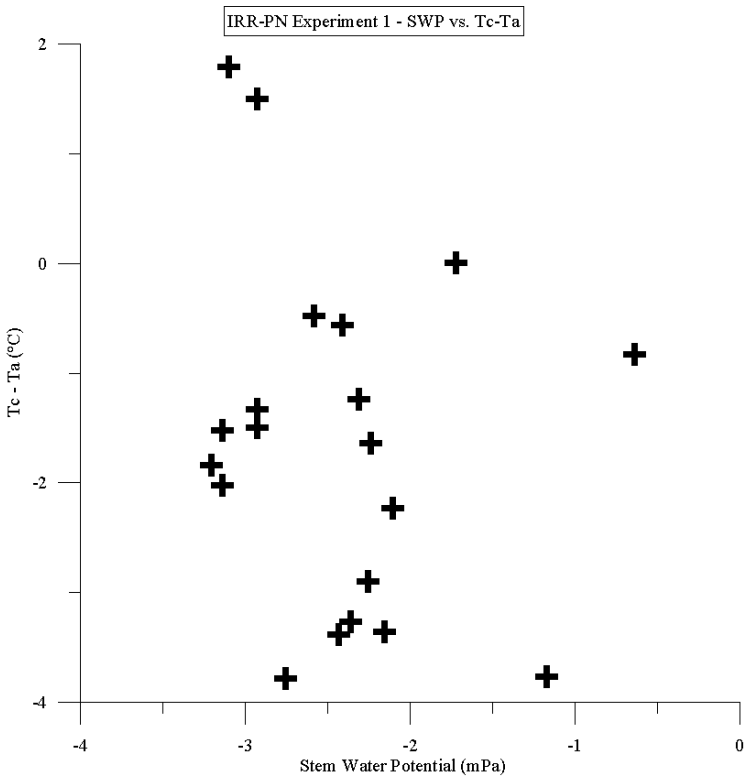

Figure 3-7. Graphical presentation of stem water potentials versus the stress-degree-day (Tc – Ta) results from measurements taken in the second infrared radiometer experiment

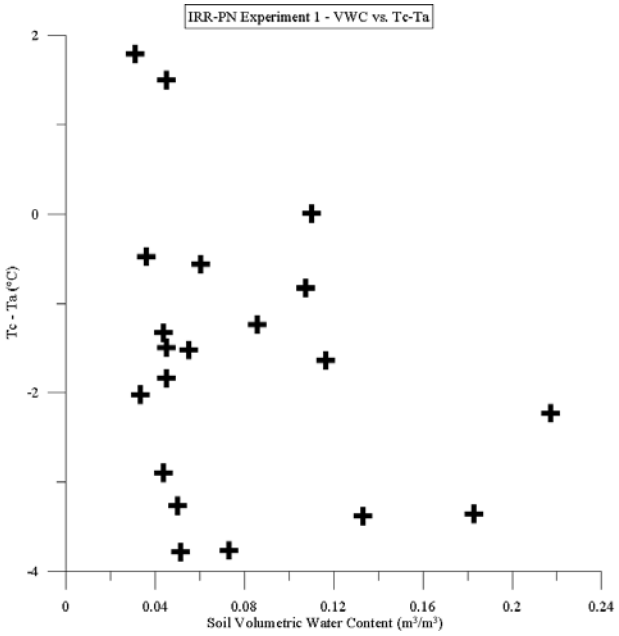

Figure 3-8. Graphical presentation of soil volumetric water content versus the stress-degree-day (Tc – Ta) results from measurements taken in the second infrared radiometer experiment

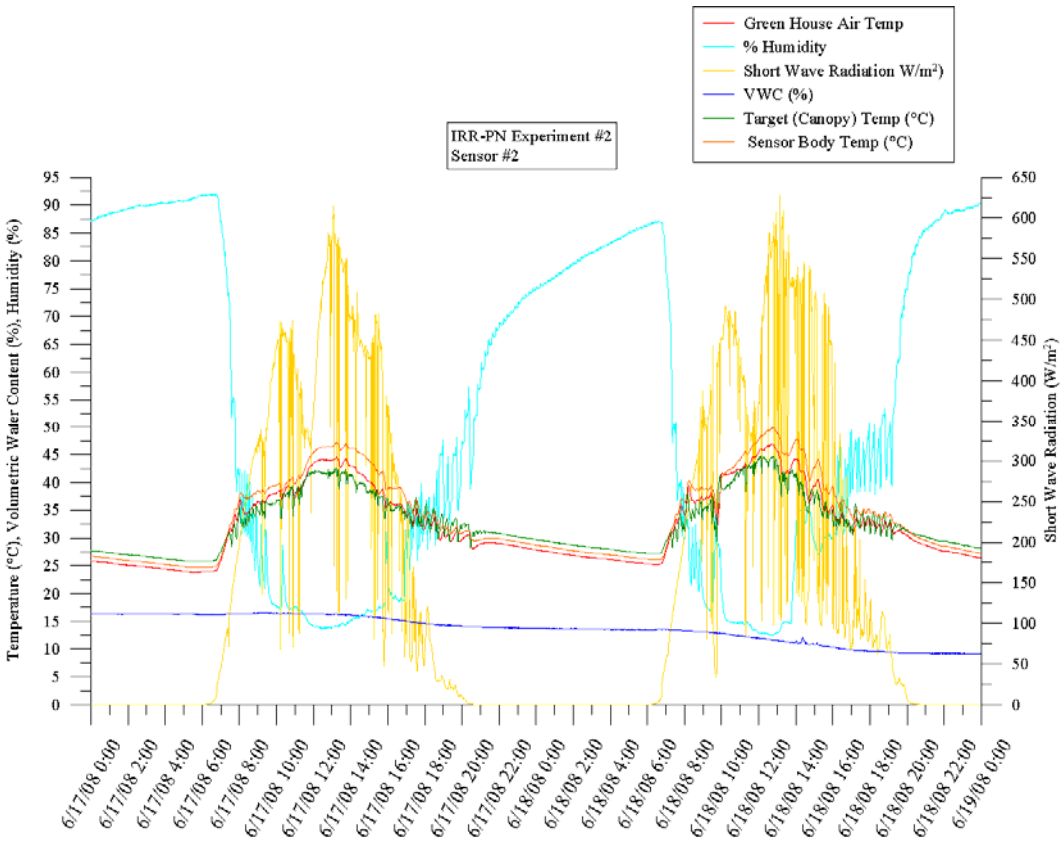

Figure 3-9. Graph of measurements taken during IRR-PN experiment 2

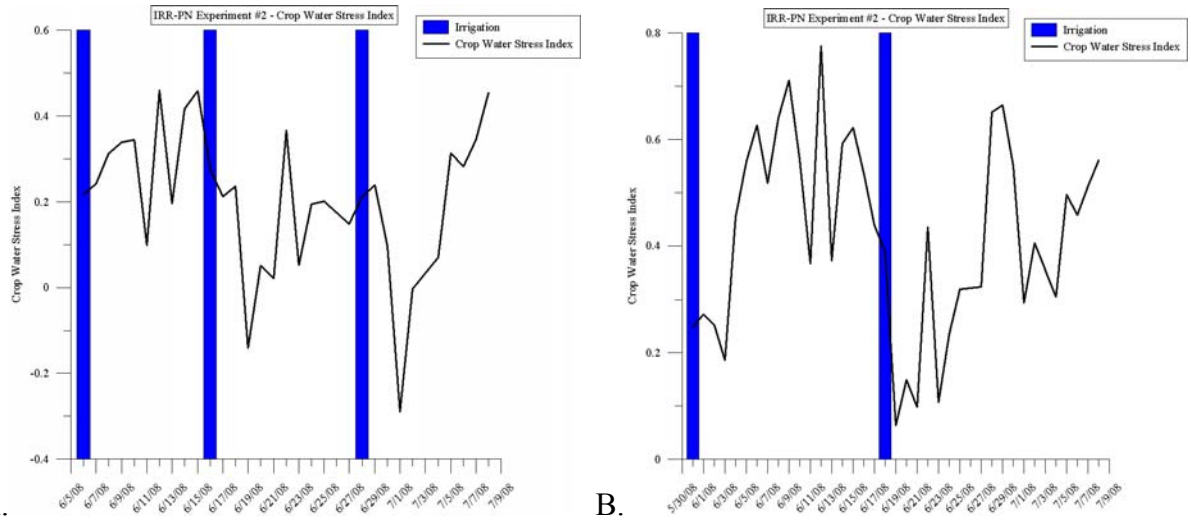

A. B.

Figure 3-10. Crop Water Stress Index and irrigation application by date. A) Rep 1, and B) Rep 2

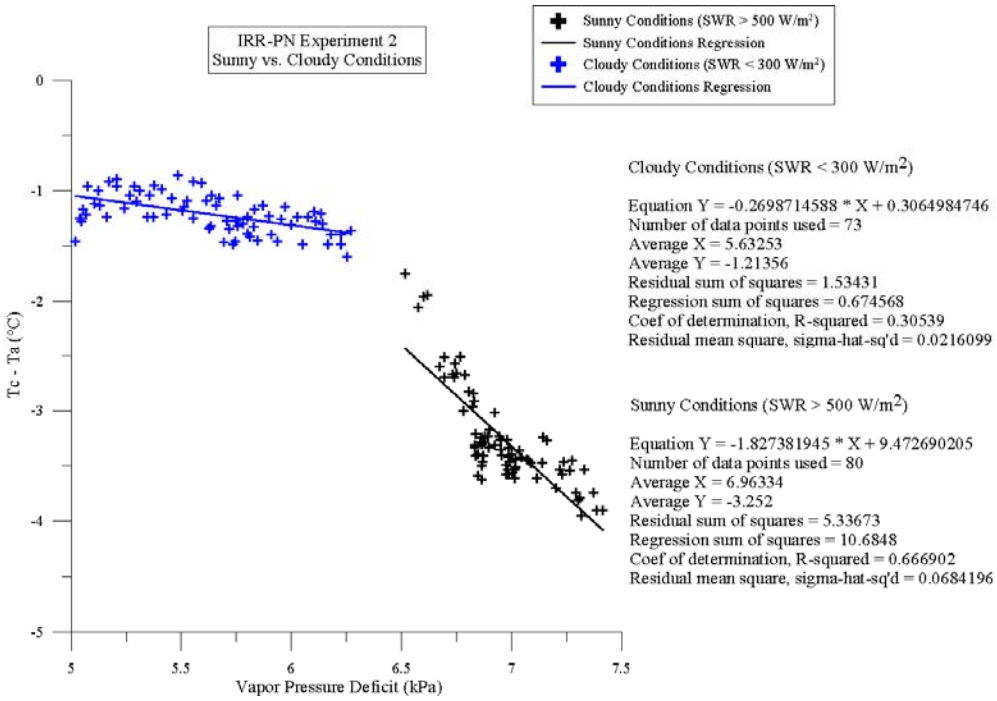

Figure 3-11. Comparison of measurements taken with the infrared radiometer in cloudy and sunny conditions in the greenhouse.

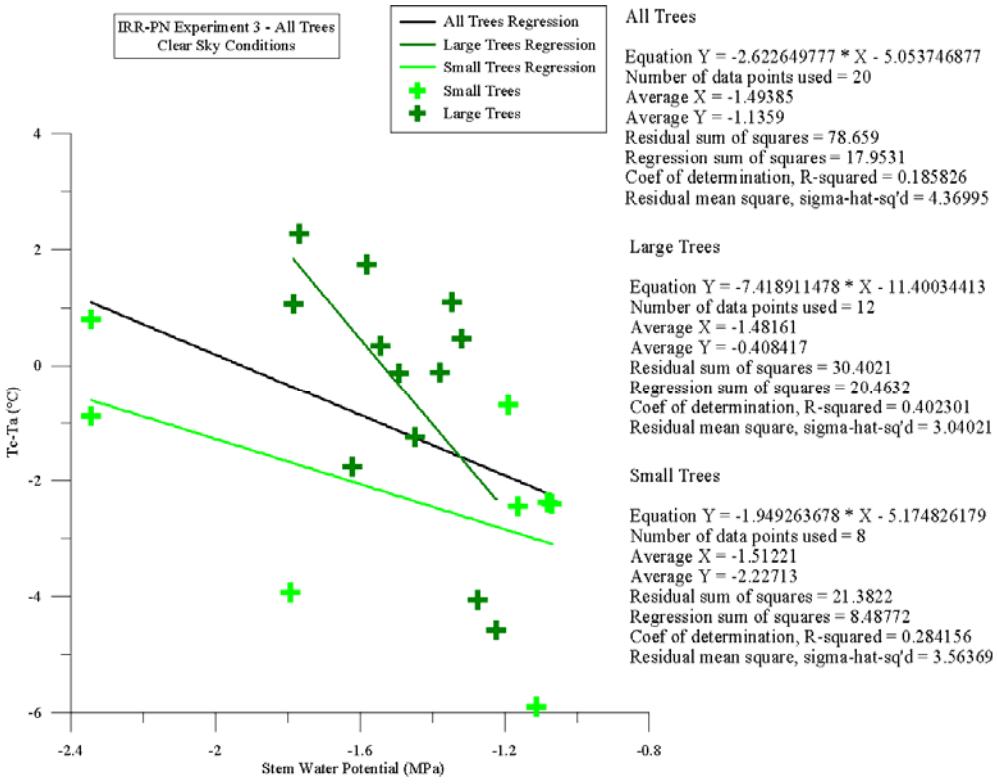

Figure 3-12. Regression analysis showing Tc – Ta versus stem water potential results from the third infrared radiometer experiment.

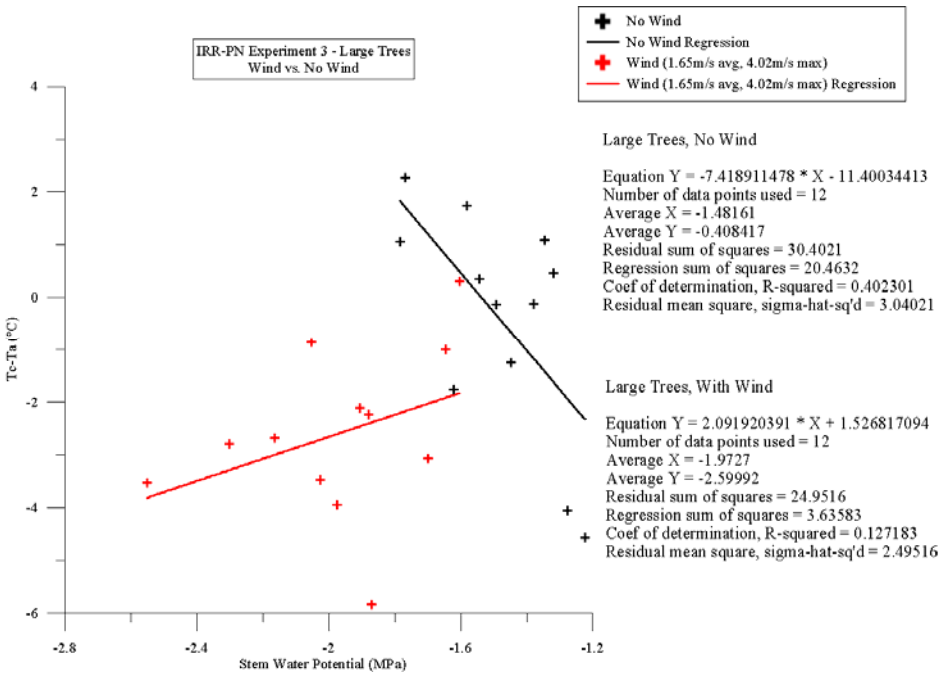

Figure 3-13. Regression analysis comparing measurements of Tc – Ta, taken with the infrared radiometer in both windy and wind free conditions versus stem water potential.

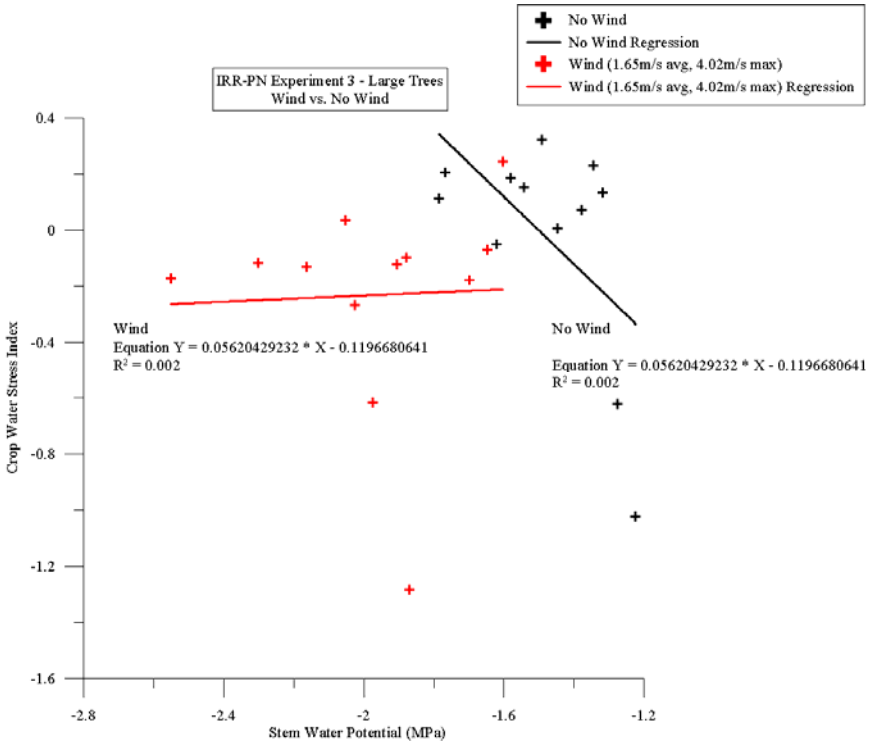

Figure 3-14. Comparison of the regression analysis of the CWSI normalized IRR-PN measurements taken in windy and windless conditions versus stem water potential

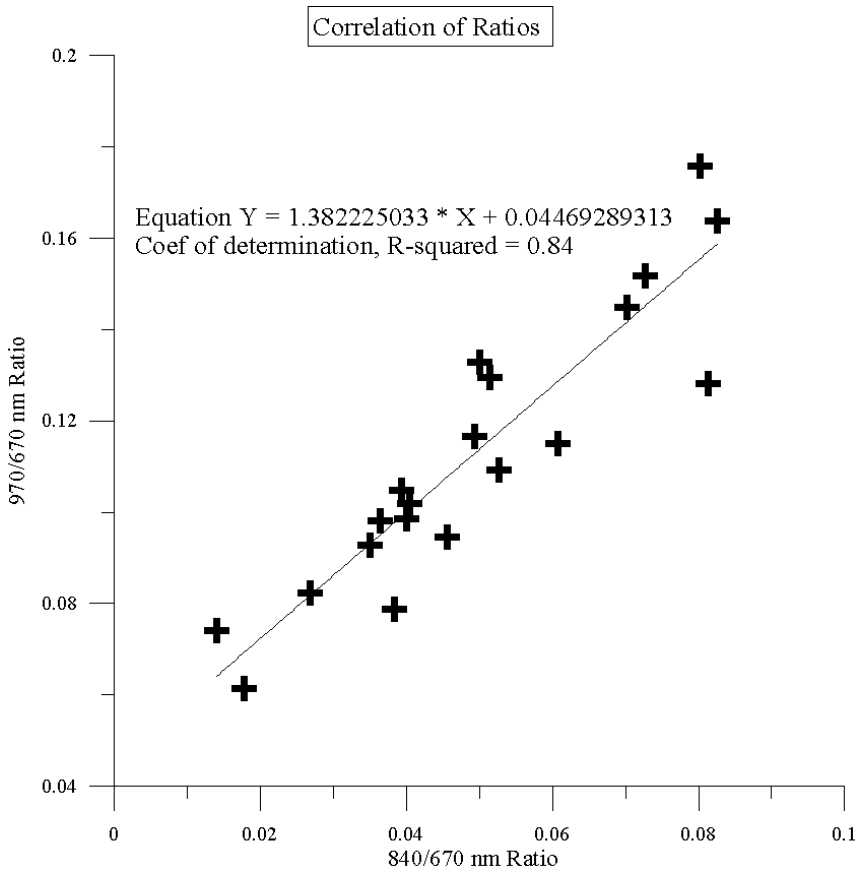

Figure 3-15. Correlation analysis of Crop Stress Index ratios using the 840 nm and 670 nm wavelengths

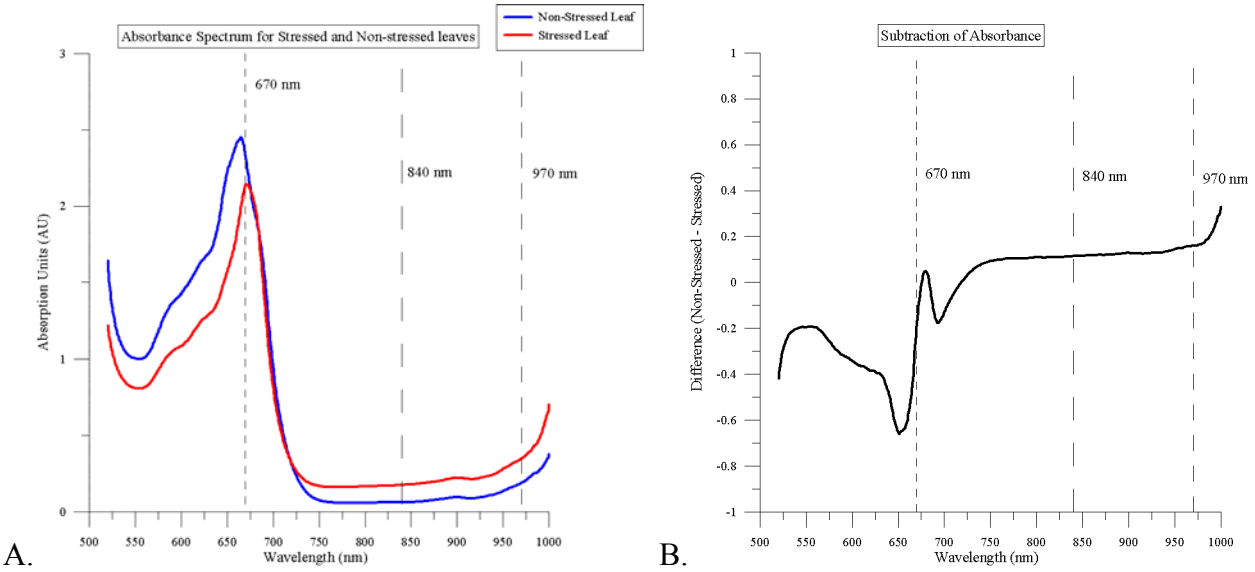

Figure 3-16. Analysis comparing the stressed and non-stressed leaves, A) measured absorption of stressed vs. non-stressed leaves and B) subtraction of absorption spectra (non-stressed – stressed)

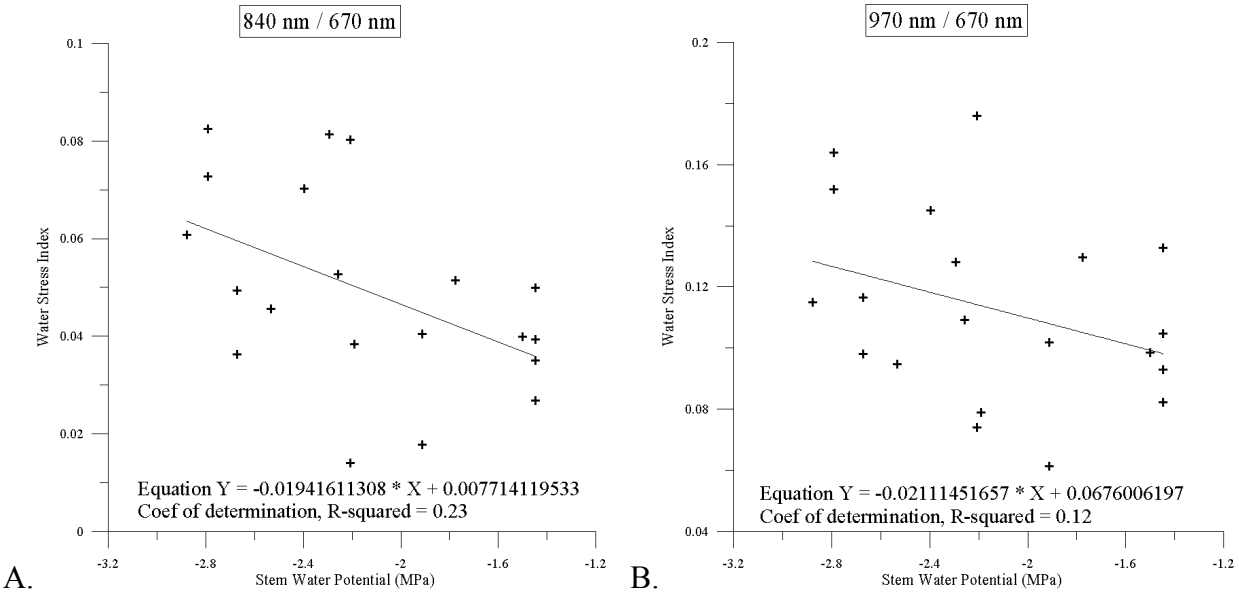

Figure 3-17. Regression analysis of water stress index ratios A) 840 nm / 670 nm and B) 970 nm / 670 nm.

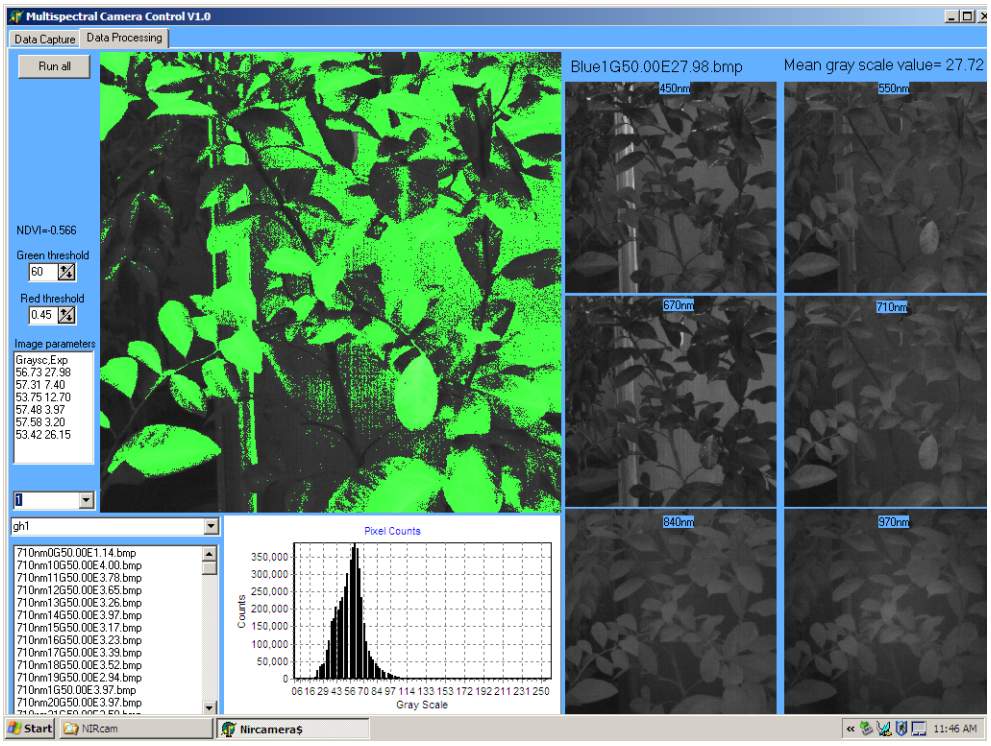

Figure 3-18. Screen capture of data processing from a small greenhouse tree showing the large amount of background interference.

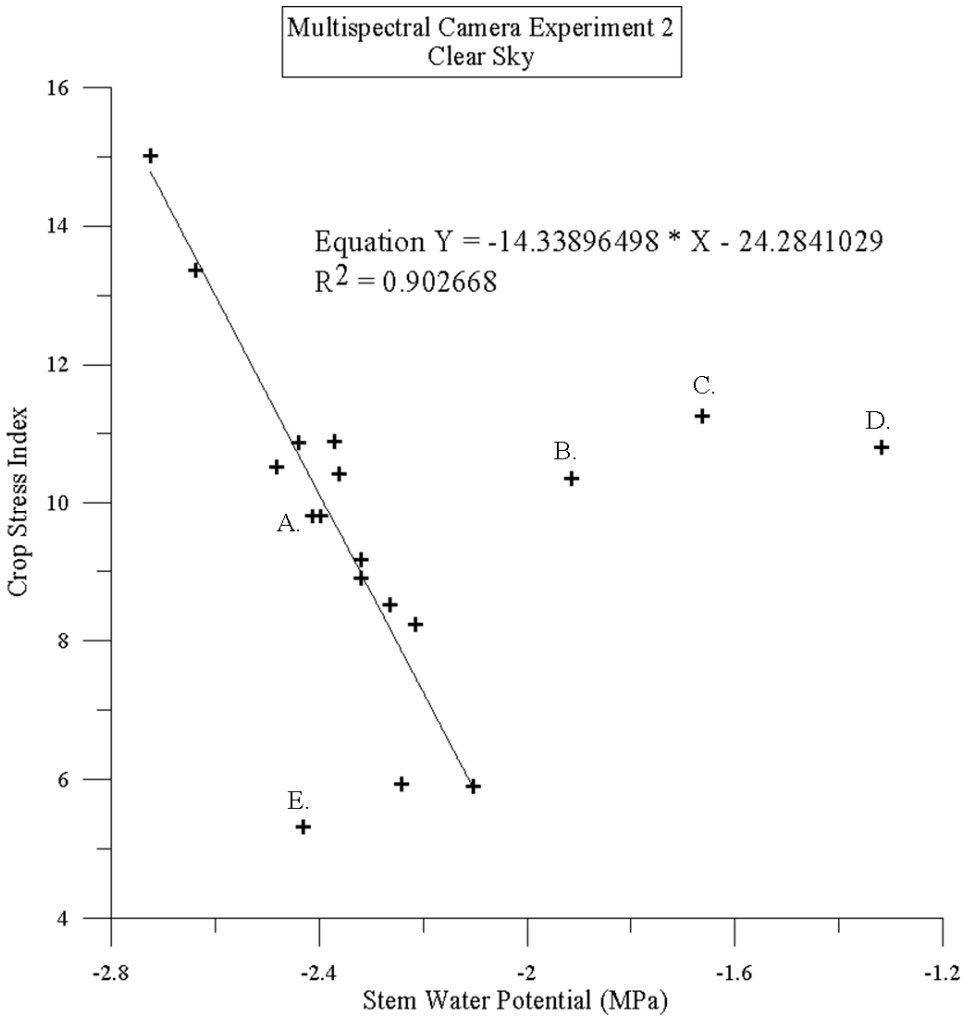

Figure 3-19. Regression from Clear Sky conditions showing outliers B. – E. as a result of improper imaging

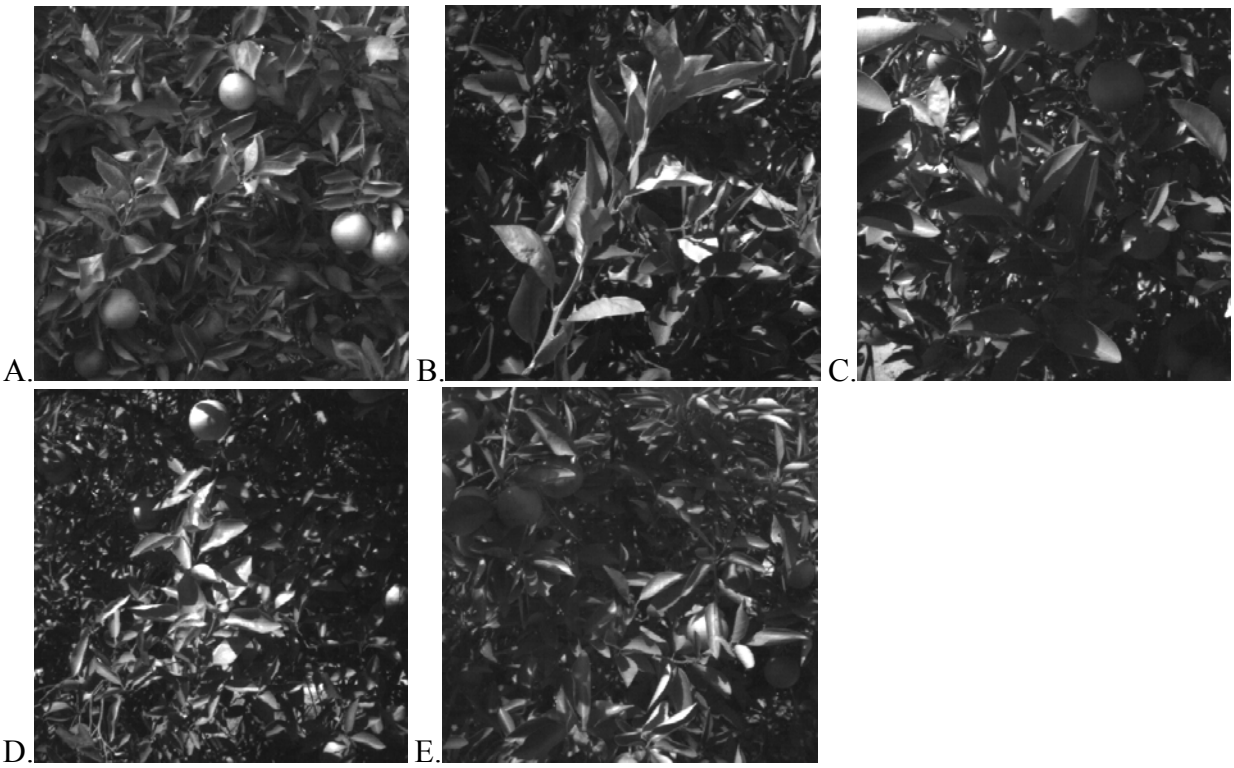

Figure 3-20. Images captured by the multispectral camera showing normal image A and outliers B – E. A) Normal capture of a uniformly sunlit canopy, no shaded holes or interfering branches, B) young light-green flush interfering with image, C) large shaded hole captured in image, D) young water stressed flush interfering with remaining image, and E) Large shaded hole in canopy.

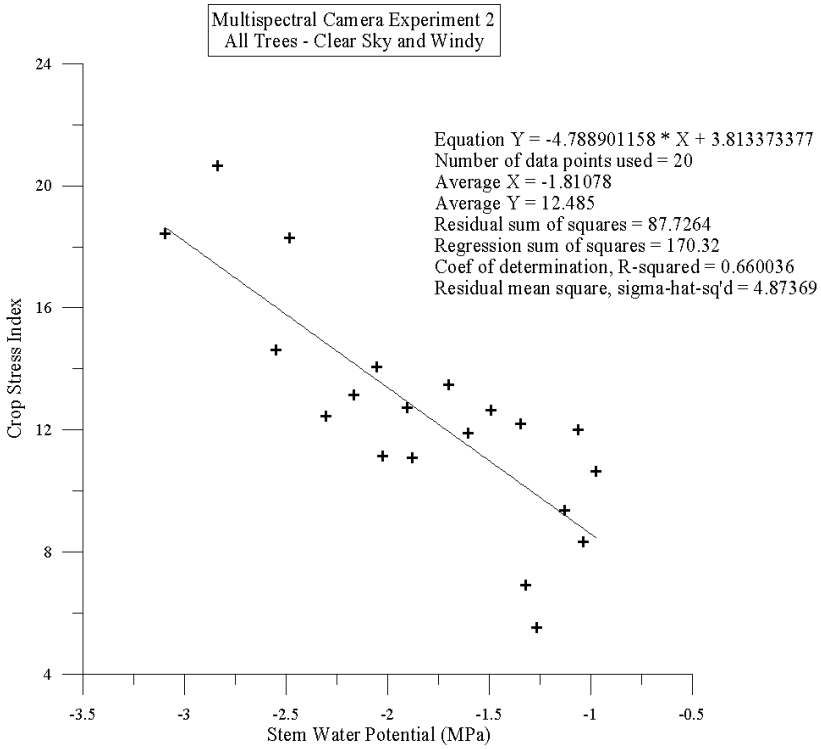

Figure 3-21. Regression analysis from measurements taken on a sunny day with average wind speed of 1.65 m/s and max gusts of 4.02 m/s.

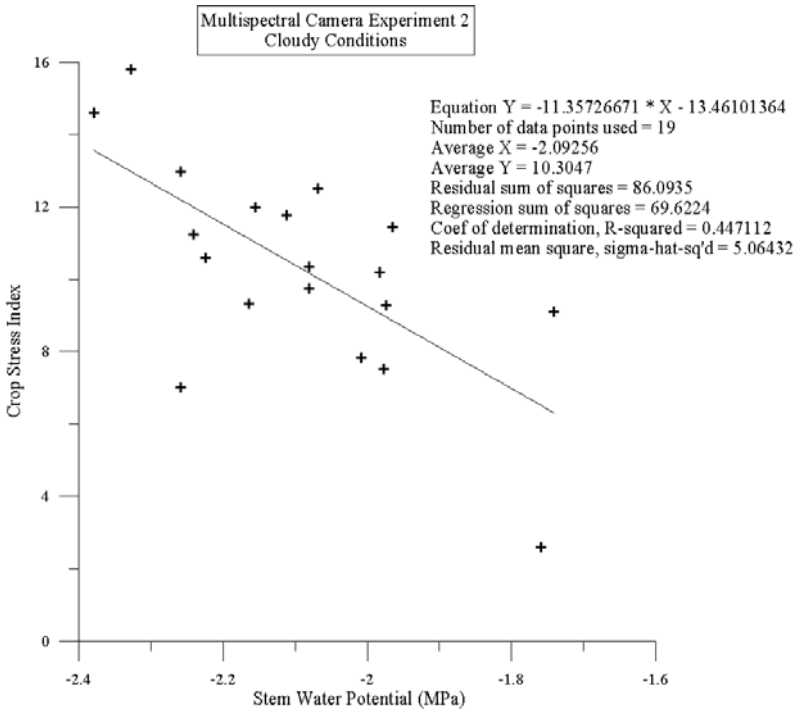

Figure 3-22. Regression analysis from measurements taken on a cloudy day

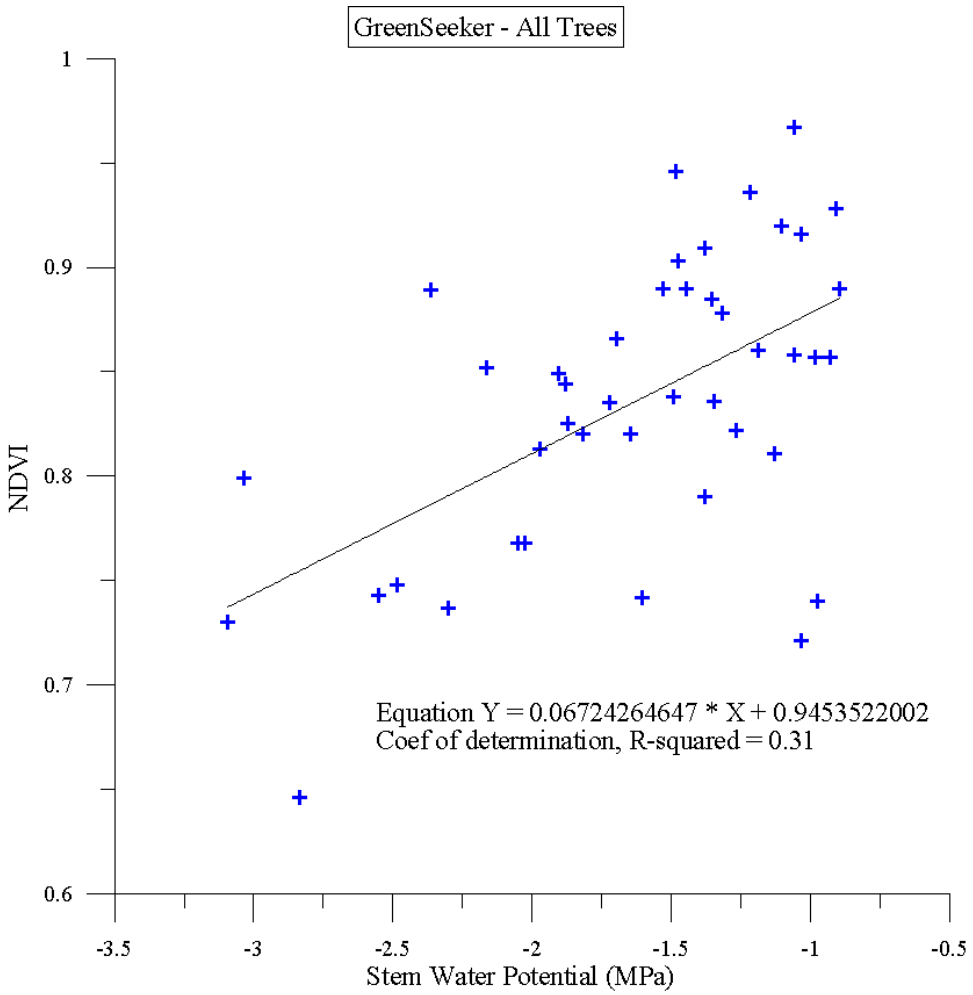

Figure 3-23. Regression analysis from measurements taken with the GreenSeeker®

CHAPTER 4
SUMMARY OF RESULTS

As water resources become limited, it is important to irrigate in the most efficient manner possible, while still maintaining a suitable crop yield. Throughout much of Florida, citrus is irrigated based on soil moisture status and evapotranspiration. However, there are several factors that contribute to a high level of variability in moisture within the rootzone. These include soil type, micro-topography, the type of irrigation system, root density, and canopy interference with rain and irrigation water, all of which make it difficult to irrigate at a high level of efficiency. Additionally, although soil moisture sensors are precise, they lack accuracy in the field due to several factors which include a small sensing volume and disruption of the soil profile required during installation. All of these factors together make questionable the accuracy of a single point soil moisture measurement to be used for irrigation scheduling. These questions of efficiency and accuracy led to the need for comprehensively mapping soil moisture variability to find how many soil based sensors would be required to efficiently irrigate trees and maintain yield.

After mapping, there was a high amount of variability in soil moisture under citrus trees after varying amounts of rainfall and irrigation, as well as after several days of drying. This spatial variability makes single point measurements inaccurate. Identifying the best position for a single moisture sensor under a citrus tree canopy for accurate irrigation scheduling is impossible, and would lead to situations of either over irrigation and leaching or possible yield reduction as a result of under irrigation. In general, recently wetted soils were more variable than drier soils. Calculations to find the number of sensors that would be needed to accurately trigger irrigation within 95% confidence of not having more than a 10% error in the plant available water (PAW) measurement, revealed that between 14 and 53 measurements were needed for dry soil conditions whereas a maximum of 289 measurements were needed for a moist soil after a rainfall

event. The lower variability in drier soils means that the moisture sensor trigger which starts the irrigation would be more reliable than the one which stops it. This also shows that the variability in the soil moisture would more often lead to situations of over irrigation rather than under irrigation since the tree is able to incorporate moisture from its entire root area. The tree would be able to utilize the water in the wetter areas of the soil even though there may be areas of soil that are dry beyond the permanent wilting point. Based on these results, using soil moisture sensors to measure volumetric water content for accurate irrigation is cost prohibitive and unfeasible. Since the aim of the Ridge Citrus BMPs is to reduce the amount of nitrogen reaching the groundwater and eventually the aquifer, more efficient irrigation triggers are necessary. Based on the mapping results, this level of irrigation control can not come from single point soil moisture measurements. As a result, canopy-based water stress methods were investigated.

Infrared canopy temperature measurements and multispectral images were tested in a controlled greenhouse environment and in a small citrus field block. In addition to testing these methods, a commercially available GreenSeeker® instrument, which is equipped with its own light source and unaffected by the amount of solar radiation was used to test the efficiency of the normalized difference vegetation index (NDVI), which is the a reflectance ratio of near infrared reflectance minus red reflectance over the near infrared reflectance plus the red reflectance (see equation, Chapter 3), in predicting plant water stress of the field trees.

Results from the thermal infrared radiometer experiment in the greenhouse, using a single air temperature (Ta) measurement subtracted from average canopy temperature (Tc) measurements (Tc – Ta) or ΔT, plotted against stem water potential (SWP), showed these measurements to be inaccurate for measuring water stress. However, due to experimental error and plant health issues, it is not possible to conclude that Tc – Ta measurements would be

inappropriate in controlled environments. After an experiment in the greenhouse to test the long term use of the infrared radiometer, it is possible to identify the water stress of the tree using the normalized Tc – Ta calculated using the crop water stress index (CWSI) (see equations, Chapter 3). Once a threshold of CWSI to plant water stress has been established, it is possible that this method could be used to schedule irrigation for potted citrus trees in a greenhouse. In the field measurements with the infrared radiometer and calculations of CWSI, variations in wind and cloud cover made reliable measurements of CWSI with thermal infrared radiometry on citrus trees impossible.

Testing the multispectral imaging method required subsequent leaf absorbance wavelength spectrum analysis. This was done to identify the appropriate ratio of reflectance wavelengths necessary for data analysis using the crop stress index (CSI), which is a ratio of reflectance at near infrared over reflectance at red. After identifying the appropriate wavelength ratio of 840 nm / 670 nm, analysis was applied to the captured images of both the greenhouse and field citrus trees using the multispectral camera. Due to the same sources of error as experienced in the greenhouse with the infrared radiometer, the multispectral camera and CSI was not effective for characterizing stress in greenhouse trees. Furthermore, the field of view for the multispectral camera at a 30 cm distance also caused error in the CSI ratio mostly due to the large amount of the background in the image that was not covered by the tree canopy in the foreground. However, results from the field experiment under clear, wind free conditions, showed that the CSI ratio was reliable at predicting the water stress of the trees ($R^2 = 0.90^{***}$). When tested under cloudy and windy conditions, the CSI ratio still provided a reasonable estimate of the tree water stress, however not to the same accuracy as seen during the clear wind free conditions (R^2

= 0.44^{**} and 0.66^{***}, respectively). It can be concluded that the multispectral camera and CSI ratio could be used to trigger irrigation once an appropriate threshold of the CSI was established.

The commercially available GreenSeeker® with NDVI output, which is unaffected by the varying levels of solar radiation, could also predict the water stress of citrus trees in the field with a statistically significant linear fit ($R^2 = 0.31^{***}$). It could be possible to schedule irrigation based on these NDVI measurements after a threshold of NDVI to SWP has been identified.

Since the tree canopy is able to integrate total water use from within the rootzone, canopy based water stress measurements would be more accurate for water stress measurements for the purpose of scheduling irrigation. It can be concluded that the infrared radiometer in the long-term greenhouse experiment and the multispectral camera and GreenSeeker® experiments in the field are more accurate for predicting water stress than using single sensor based soil moisture measurements to schedule irrigation.

LIST OF REFERENCES

Alados, I., F.J. Olmo, I. Foyo-Moreno, and L. Alados-Arboledas. 2000. Estimation of photosynthetically active radiation under cloudy conditions. *Agricultural and Forest Meteorology*. 102: 39-50.

Alva, A.K., O. Prakash, A. Fares, and G. Hornsby. 1999. Distribution of rainfall and soil moisture content in the soil profile under citrus tree canopy and at the dripline. *Irrigation Science.* 18: 109-115.

Boman, B.J. and E.W. Stover. 2002. Managing salinity in Florida citrus. University of Florida, IFAS Cooperative Extension Service. CIR 1411.

Burrough, P.A. and R.A. McDonnell. *Principles of Geographical Information Systems.* 333 pp. Oxford University Press Inc., New York. 2004.

Campbell, G.S. and W.H. Gardner. 1971. Psychrometric measurement of soil water potential: temperature and bulk density effects. *Proceedings of the Soil Science Society of America.* 35: 8-12.

Charlesworth, P. 2000. Soil water monitoring. *National Program for Irrigation Research and Development.* 101 pp. CSIRO Land and Water, Canberra, Australia.

Cohen, Y., V. Alchanatis, M. Meron, Y. Saranga and J. Tsipris. 2005. Estimation of leaf water potential by thermal imagery and spatial analysis. *Journal of Experimental Botany* 56(417): 1843-1852.

Curran, P.J. 1983. Multispectral remote sensing for the estimation of green leaf area index. *Philosophical Transactions of the Royal Society A* 309:257-270.

Dallon, D. and B. Bugbee. 2003. Measurement of water stress: comparison of reflectance at 970 and 1450. Utah State University, Crop Physiology Laboratory. http://www.usu.edu/cpl/PDF/Water%20Stress_Dallon.pdf. Last accessed March 4, 2009.

Dane, J.H. and G.C. Topp. 2002. The soil solution phase. J.H. Dane and G.C. Topp. *Methods of soil analysis, Part 4: Physical methods.* Soil Science Society of America, Inc. Madison, WI.

Davis, J.L. and A.P. Annan. 2002. Ground penetrating radar to measure soil water content. 446-463. J.H. Dane and G.C. Topp. *Methods of soil analysis, Part 4: Physical Methods.* Soil Science Society of America, Inc. Madison, WI.

Elvidge, C.D. and Z. Chen. 1995. Comparison of broad-band and narrow-band red and near-infrared vegetation indices. *Remote Sensing of Environment*. 54:1 38-48.

Gamma Design Software. 2004. *GS+:Geostatistics for the Environmental Sciences.* Gamma Design Software, Plainwell, Michigan USA.

González-Dugo, M.P., M.S. Moran, L. Mateos, and R. Bryant. 2006. Canopy temperature variability as an indicator of crop water stress severity. *Irrigation Science* 24(4):233-240.

Haman, D.Z. and F.T. Izuno. 1993. Soil plant water relationships. Univ. of Florida, IFAS Coop. Ext. Serv.CIR1085.

Hope, A.S. and R.D. Jackson. 1989. Early morning canopy temperatures for evaluating water stress in a wheat crop. *Water Resources Bulletin: American Water Resources Association* 25(5):1009-1014.

Idso, S.B., R.D. Jackson, P.J. Pinter, Jr., R.J. Reginato and J.L. Hatfield. 1981. Normalizing the stress-degree-day parameter for environmental variability. *Agricultural Meteorology.* 24: 45-55.

Jackson, R.D. 1982. Canopy temperature and crop water stress. *Advances in Irrigation* 1:43-85.

Jackson, R.D., S.B. Idso, R.J. Reginato, and P.J. Pinter, Jr. 1981. Canopy temperature as a crop water stress indicator. *Water Resources Research* 17(4):1133-1138.

Jackson, R.D., W.P. Kustas, and B.J. Choudhury. 1988. A reexamination of the crop water stress index. *Irrigation Science* 9:309-317.

Jones, H.G. 2004. Irrigation scheduling: advantages and pitfalls of plant-based methods. *Journal of Experimental Botany.* 55(407):2427-2436.

Jones, H.G. 2007. Monitoring plant and soil water status: established and novel methods revisited and their relevance to studies of drought tolerance. *Journal of Experimental Botany.*58(2): 119-130.

Leinonen, I., and H.G. Jones. 2004. Combining thermal and visible imagery for estimating canopy temperature and identifying plant stress. *Journal of Experimental Botany.* 55(401): 1423-1431.

McCutchan, H. and K.A. Shackel. 1992. Stem-water potential as a Sensitive indicator of water stress in prune trees (*Prunus domestica* L. cv. French). *Journal of the American Society for Horticultural Science.* 117(4): 607-611.

Möller, M., V. Alchanatis, Y. Cohen, M. Meron, J. Tsipris, A. Naor, V. Ostrovsky, M. Sprintsin, and S. Cohen. 2007. Use of thermal and visible imagery for estimating crop water status of irrigated grapevine. *Journal of Experimental Botany.* 58(4): 827-838.

Monteith, J.L. and M.H. Unsworth. *Principles of Environmental Physics 3rd Edition.* 418 pp. Elsevier, London. 2008.

Morgan K., H. Beck, J. Scholberg, and S. Grunwald. 2006. In-season irrigation and nutrient decision suport system for citrus production. World Congress on Computers in Agriculture, Orlando, FL, July 24-26, 2006.

Mulla, D.J. and A.B. McBratney. 2000. Soil spatial variability. A:321–352. M.E. Summer. *Handbook of Soil Science.* CRC Press. Boca Raton.

Muñoz-Carpena, R. 2004. Field Devices for monitoring soil water content. *Department of Agricultural and Biological Engineering.* University of Florida Cooperative Extension Service. Bulletin 343.

NOAA, Southern Region Headquarters. 2008. Vapor Pressure. http://www.srh.noaa.gov/sju/Climate/wxcalc2go/formulas/vaporPressure.html. Last accessed March 19, 2009.

Robinson, D.A., C.M.K. Gardner and J.D. Cooper. 1999. Measurement of relative permittivity in sandy soils using TDR, capacitance and theta probe: comparison, including the effect of bulk soil electrical conductivity. *Journal of Hydrology*. 223: 198-211.

Schmitz, M. and H. Sourell. 2000. Variability in soil moisture. *Irrigation Science.* 19: 147-151.

Scholander, P., H. Hammel, E.Y. Bradstreet, and E. Hemmingsen. 1965. Sap pressure in vascular plants. *Science*. 37: 247-274.

Schumann, A.W., K. Hostler, J.C. Melgar, and J. Syvertsen. 2007. Georeferenced ground photography of citrus orchards to estimate yield and plant stress for variable rate technology. *Proceedings of the Florida State Horticulture Society.* 120: 56-63.

Southwest Florida Water Management District. 2002. GIS Data, SOILS. http://www.swfwmd.state.fl.us/data/gis/libraries/physical_dense/soils.htm. Last accessed March 19, 2009.

Topp, G. C., J. L. Davis, and A. P. Annan. 1980. Electromagnetic Determination of Soil Water Content: Measurements in Coaxial Transmission Lines, *Water Resource Research.* 16(3): 574–582.

Wijaya, K., T. Nishimura and K. Makoto. 2002. Estimation of bulk density of soil by using amplitude domain reflectometry (ADR) probe. *17th World Congress of Soil Science.* Thailand. 385.

U.S. Water Conservation Laboratory. 2001. Thermal Crop Water Stress Indices. http://www.plantstress.com/articles/drought_i/drought_i_files/CWSI_phoenix.pdf. Last accessed March 10, 2009

USDA-NRCS. 1990. Soil survey of Polk County, Florida. 235. USDA

BIOGRAPHICAL SKETCH

Laura Waldo was born in Madison, Wisconsin and moved to Florida in 1982. Upon graduating from Dr. Phillips High School in Orlando, FL, she attended Valencia Community College and earned a general education Associate in Arts degree in 2001. Immediately following, she attended Florida Southern College-Lakeland, FL and earned a Bachelor of Science degree in horticulture science in 2003. In April of 2004 she began work on the Ridge Citrus nitrogen BMP verification study at the UF IFAS Citrus Research and Education Center-Lake Alfred, FL. In the fall of 2006, she began her Master of Science degree at the University of Florida-Gainesville, FL in the department of Soil and Water Science as a distance education student, while working in Lake Alfred. In 2007, she became a Graduate Assistant while finishing her thesis research. She completed her Master of Science degree in Soil and Water Science in 2009.